

GENETIC BASIS OF DISTAL ARTHROGRYPOSES

by

Reha Toydemir

A dissertation submitted to the faculty of  
The University of Utah  
in partial fulfillment of the requirements for the degree of

Doctor of Philosophy

Department of Human Genetics

The University of Utah

December 2006

Copyright © Reha Toydemir 2006

All Rights Reserved




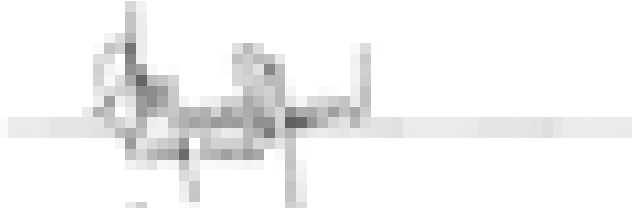






THE UNIVERSITY OF UTAH GRADUATE SCHOOL

**SUPERVISORY COMMITTEE APPROVAL**

of a dissertation submitted by

Reha Toydemir

This dissertation has been read by each member of the following supervisory committee and by majority vote has been found to be satisfactory.

	 Chair: Michael Bamshad
	
	
	 James
	 Anne Moon

THE UNIVERSITY OF UTAH GRADUATE SCHOOL

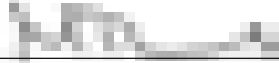
**FINAL READING APPROVAL**

To the Graduate Council of the University of Utah:

I have read the dissertation of Reha Toydemir in its final form and have found that (1) its format, citations, and bibliographic style are consistent and acceptable; (2) its illustrative materials including figures, tables, and charts are in place; and (3) the final manuscript is satisfactory to the supervisory committee and is ready for submission to The Graduate School.

  
\_\_\_\_\_

Date

  
\_\_\_\_\_

Michael Bamshad

Chair: Supervisory Committee

Approved for the Major Department

  
\_\_\_\_\_  
  
\_\_\_\_\_  
  
\_\_\_\_\_

  
\_\_\_\_\_  
  
\_\_\_\_\_  
  
\_\_\_\_\_

Approved for the Graduate Council

  
\_\_\_\_\_

David S. Chapman  
Dean of The Graduate School

## ABSTRACT

Every year millions of children are born with a birth defect. Birth defects, which can be described as abnormalities of structure or function that is present from birth, are the leading cause of infant death in developed countries and a significant cause of morbidity and economic burden in low- or middle-income countries. This dissertation addresses the genetic basis of distal arthrogryposes (DAs), a subgroup of birth defects that are characterized by contractures of the distal joints of a limb.

Based on previous research of our laboratory, we hypothesized that DAs are defects of contractile apparatus in fast twitch skeletal myofibers and tested this hypothesis in four DA syndromes. We found that mutations of the embryonic myosin heavy chain gene cause DA2A and DA2B, whereas a missense mutation of the perinatal myosin heavy chain gene is responsible for DA7. Furthermore, we found mutations in the adult and extraocular myosin heavy chain genes in some DA5 patients.

Furthermore, we noticed some patients with similar findings who do not meet the diagnostic criteria of the known DA syndromes. We proposed one of these conditions to be named as DA10, and mapped this condition to the long arm of chromosome 2. We named the other condition as the CATSHL syndrome, which we showed to be caused by a loss-of-function mutation in the fibroblast growth factor receptor 3 gene.

The main contribution of this research is to benefit affected individuals and their families, since molecular testing can now be offered to them. In addition, through

further studies leading to a better understanding of normal and abnormal development, effective strategies for prevention and treatment of congenital limb malformations can be developed.

## TABLE OF CONTENTS

ABSTRACT.....	iv
ACKNOWLEDGMENTS.....	viii
CHAPTER	
1. INTRODUCTION.....	1
References.....	13
2. MUTATIONS IN EMBRYONIC MYOSIN HEAVY CHAIN (MYH3) CAUSE FREEMAN-SHELDON SYNDROME AND SHELDON-HALL SYNDROME.....	16
Methods.....	20
References.....	21
3. TRISMUS-PSEUDOCAMPTODACTYLY SYNDROME IS CAUSED BY A RECURRENT MUTATION IN <i>MYH8</i> .....	27
Introduction.....	28
Subjects and methods.....	29
Results.....	30
Discussion.....	31
References.....	33
4. A LOSS-OF-FUNCTION MUTATION IN FGFR3 CAUSES CAMPTODACTYLY, TALL STATURE, AND HEARING LOSS (CATSHL) SYNDROME.....	35
References.....	41
APPENDICES	
A. DISTAL ARTHROGRYPOSIS TYPE 5 IS CAUSED BY DEFECTS OF MYOSIN.....	52

B. A NEW AUTOSOMAL DOMINANT DISTAL ARTHROGRYPOSIS  
SYNDROME CHARACTERIZED BY PLANTAR TENDON CONTRACTURES  
IN A LARGE UTAH KINDRED MAPS TO 2q.....55



## ACKNOWLEDGMENTS

I would like to thank my advisor Michael J. Bamshad for giving me the opportunity to work in his laboratory and helping me develop as an independent scientist. I also wish to thank him for providing the clinical and laboratory resources I needed.

I am indebted to Lynn B. Jorde for his continuous and unconditional support. I am grateful to the members of my committee, Suzanne Mansour, James Metherall, and Anne Moon, for their time, advice and encouragement throughout my graduate career.

This work would not be possible without the help of many collaborators. Drs. John Carey, David Viskochil, David Stevenson, and many other clinicians have provided phenotypic analyses. The past and present members of the Bamshad and Jorde labs provided encouragement and everyday advice. Frank Whitby helped me interpret the potential effects of the mutations on protein structure and function. The Sequencing and Genotyping Core Facilities helped me make my discoveries faster. Kevin Hurst and other members of the IT department deserve my thanks for their support.

I am thankful to the individuals with congenital contractures and their families who volunteered their time, blood, and tissues. I appreciate the funding from the University of Utah Graduate School as well as the grants from National Institutes of Health and Center for Disease Control. I would like to thank to the journals Nature

Genetics, American Journal of Medical Genetics, and American Journal of Human Genetics, for publishing my work and allowing me to use reprints.

I want to thank my parents Necla and İlhan Toydemir and my brother Suha, for their constant support. I will always appreciate their love and the encouraging environment they provided. Finally, I want to thank my wife Pınar, for all the support she gave me during my career; and the boys, Ada and Doruk, for giving us joy and happiness.

## CHAPTER 1

### INTRODUCTION

Every year more than 8 million children are born with a birth defect.<sup>1</sup> Also known as congenital malformations, birth defects are a global problem. They are the leading cause of infant death in developed countries.<sup>1</sup> However, their impact is more severe in low- or middle-income countries, since birth defects cause a significant morbidity and economic burden.

Birth defects, in general, can be described as abnormalities of structure or function that are present from birth. They may or may not be clinically obvious at birth; sometimes they can be diagnosed only later in life. More than 7000 types of birth defects have been identified to date.<sup>1</sup> The most common birth defects affect the heart, the central nervous system and the musculoskeletal system, including the limbs.<sup>1</sup>

Congenital limb malformations are the second most frequent structural birth defects in humans.<sup>1</sup> The phenotypic spectrum of limb malformations can be very wide, ranging from subtle changes in morphology to aberrant patterning or complete absence of a limb. Mutations of more than two dozen genes are known to cause these limb malformations, underscoring the importance of expression of these genes in the correct place at the correct time for proper limb development and differentiation.

Vertebrate limbs develop from small buds that contain undifferentiated mesoderm (mesenchyme) cells.<sup>2</sup> These buds differentiate simultaneously with outgrowth and eventually form specific limb structures. In human embryos, the first sign of a limb is seen at around 28 days, and the major structures of the limbs are fully present by the 8<sup>th</sup> week.<sup>2</sup> Despite extensive efforts from researchers in many fields of biomedicine, the exact mechanism by which individual limb structures are formed in proper places and how their growth is regulated is still not clear.

When a mutation is found to be the cause of a congenital malformation, the normal function of the mutated gene can be interpolated based on the observed phenotype. Thus, the results of such studies, combined with the accumulating knowledge of normal development, might lead to improved patient care including better diagnosis, counseling, prevention, and therapeutic options.

Research presented in this dissertation addresses the genetic basis of a subgroup of congenital malformation disorders, the distal arthrogryposes (DA). Distal arthrogryposes are a group of autosomal dominant disorders characterized by congenital contractures of the distal joints of a limb and limited proximal joint involvement, without primary neurological defects affecting the limbs.<sup>3</sup> The extended classification of distal arthrogryposes includes 10 different syndromes<sup>3</sup> (Table 1.1). In this classification, the distinguishing findings observed consistently in individuals affected with each syndrome were used to group these conditions, and DAs with more similar findings were grouped together.

Table 1.1. The revised and extended classification of distal arthrogryposes.

Name	Other names	Unique findings	Ref.
DA1	Digitolar dysmorphism	Camptodactyly Clubfoot Dislocated hips	4, 5
DA2A	Freeman-Sheldon S. Whistling Face S. Windmill Vane Hand S. Craniocarpotarsal Dystrophy	Severe contractures of facial muscles Scoliosis	6
DA2B	Sheldon-Hall S.	Mild contractures of facial muscles	7
DA3	Gordon S.	Cleft palate Short stature	5, 8, 9
DA4	-	Scoliosis	5, 10
DA5	Oculomelic Amyoplasia	Ophthalmoplegia Ptosis	11
DA6	-	Sensorineural hearing loss	12
DA7	Hecht-Beals S. Dutch Kentucky S.	Trismus Pseudocamptodactyly	13, 14
DA8	Dominant Pterygium S.	Multiple pterygia	15
DA9	Beals-Hecht S. Contractural Arachnodactyly	Tall stature Arachnodactyly Crumpled ears	16

All DA syndromes have autosomal dominant inheritance and show phenotypic variability, even within families. Except for individuals with DA4 (OMIM 609128), intelligence is not affected in these conditions. Distal arthrogyriposis type 1 (DA1, OMIM 108120) is the DA group with only distal limb contractures. Other DA syndromes have unique findings in addition to distal joint contractures. Contractures of the orofacial muscles are characteristic of DA2A (severe, OMIM 193700) and DA2B (mild, OMIM 601680). Cleft palate is usually seen in DA3 (OMIM 114300), whereas extraocular muscles are affected in DA5 (OMIM 108145). DA6 (OMIM 108200) is associated with camptodactyly and sensorineural hearing loss. Individuals affected with DA7 (OMIM 158300) also have camptodactyly; however, it occurs only with dorsoflexion of the hands and is hence called ‘pseudocamptodactyly’. These patients also have difficulty in fully opening their mouth. Individuals affected with DA8 (OMIM 178110) have multiple pterygia involving the neck, knees, elbows, and the axilla. Finally, DA9 (OMIM 121050) is characterized by a marfanoid habitus, arachnodactyly, “crumpled” ears, and some cardiac abnormalities.

Previous research attempting to understand the genetic basis of distal arthrogyriposis syndromes led to the identification of mutations in several families. Mutations in the gene encoding fibrillin 2 (*FBN2*) were shown to cause DA9.<sup>17</sup> Fibrillin is a major component of the extracellular matrix. Mutations in fibrillin 1 (*FBN1*), a member of the same gene family, cause Marfan syndrome, in which heart and eye problems as well as arachnodactyly (similar to DA9) occur.<sup>15</sup> More recently, a mutation affecting the skeletal tropomyosin-beta gene (*TPM2*) was shown to occur in a DA1 family,<sup>18</sup> and mutations in the genes encoding the fast twitch skeletal muscle

isoforms of troponin I (*TNNI2*) and troponin T (*TNNT3*) were shown, by our lab, to cause some cases of DA2B.<sup>18,19</sup>

The initial work completed in our lab failed to account for the majority of DA cases. However, it led to the hypothesis that DAs are defects of the contractile apparatus in fast-twitch skeletal myofibers (Figure 1.1). I have tested this hypothesis by utilizing a candidate gene approach to find the molecular genetic basis of several DA syndromes. The general approach to these studies included recruiting families with these disorders, constructing pedigrees, and evaluating the clinical phenotypes of affected individuals.

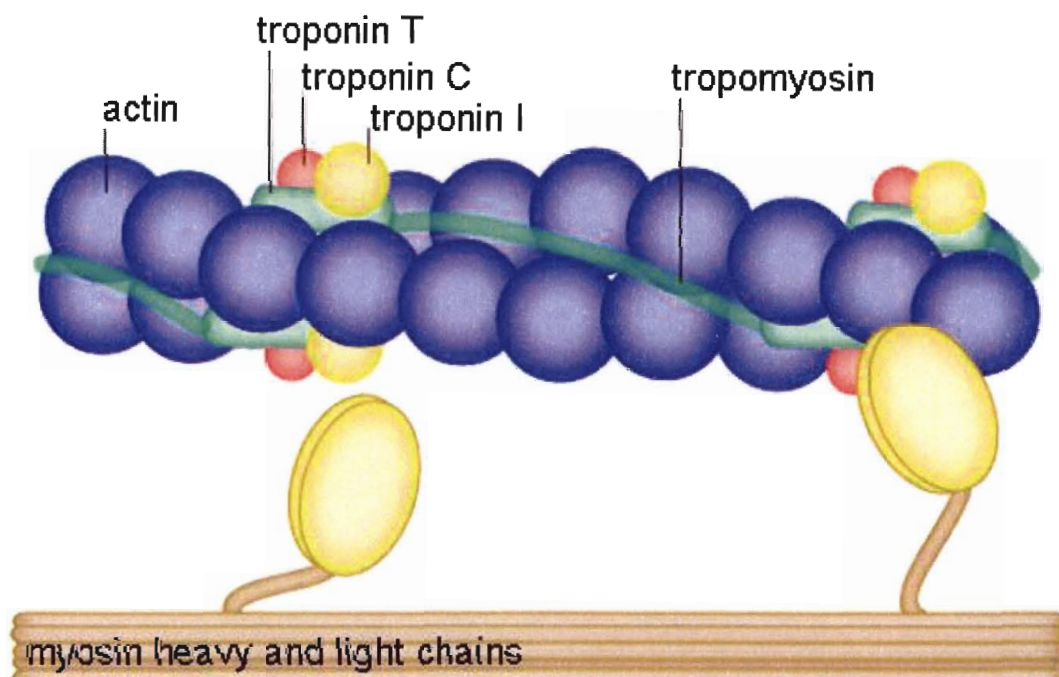


Figure 1.1. Schematic representation of the contractile apparatus in skeletal muscles. Tropomyosin and troponin molecules together with the actin polymer form the thin filament. The regulatory and essential myosin light chains with the myosin heavy chain molecules form the thick filament.

Once the patients and families were classified into relevant DA groups, I took a functional candidate gene approach to identify the genes, which, when mutated, result in the respective DA syndromes. One of the major, and relatively less studied, components of the skeletal apparatus is the myosin chains. Myosins are ubiquitous motor proteins. They use ATP hydrolysis to convert chemical energy to mechanical force. The muscle myosin is a hexamer consisting of two heavy chains and two pairs of light chains (essential and regulatory light chains). In humans, six skeletal myosin heavy chain genes have been characterized. All skeletal myosin heavy chain genes are clustered in the short arm of chromosome 17 (Figure 1.2). Although not very well characterized in humans, the spatiotemporal expression pattern and the energy utilization and force production behavior of these genes are slightly different.<sup>20</sup> *MYH3* expression starts during the embryonic period and is followed by *MYH4* and *MYH8* expression in the fetal and perinatal periods, respectively.<sup>20</sup> *MYH1* and *MYH2* are mainly expressed in adult skeletal muscles, and *MYH13* is strongly expressed in extraocular muscles.<sup>20</sup> Since all DA patients have contractures at the time of birth, I focused on the MYH genes that are expressed early in development (i.e., embryonic, fetal and perinatal myosin heavy chain genes).



Figure 1.2. Genomic organization of the skeletal myosin heavy chain genes on the short arm of chromosome 17.



This dissertation is a collection of studies on four different syndromes. In Chapter 2, I present my data showing that mutations of the embryonic myosin heavy chain (*MYH3*) gene cause about 95% of DA2A cases and one-third of DA2B cases. These two conditions are caused by different mutations (except p.T178I found in both DA2A and DA2B cases). In general, mutations causing DA2A were localized near the ATP binding site of the myosin head, whereas mutations causing DA2B were often on the outer parts of the exposed to the surface. The importance of this finding remains to be determined. DA2B seems to be more heterogeneous genetically, since mutations in *TNNI2* and *TNNT3* can also cause DA2B, but altogether mutations of these three genes account for only half of the cases.

In Chapter 3, I present my results showing that a missense mutation of the perinatal myosin heavy chain (*MYH8*) gene is responsible for all DA7 cases. Moreover, I show that the same missense mutation arose on two genetic backgrounds, arguing against a founder effect and suggesting that DA7 families do not share a recent common ancestor.

Previously it has been suggested that the same missense mutation (p.R674Q) is the cause of a variant form of Carney Complex,<sup>21</sup> a multiple neoplasia syndrome in which affected individuals also have freckles and cardiac myxomas.<sup>22</sup> After finding the p.R674Q mutation in a family with features of both Carney complex and DA7, Veugelers and colleagues suggested that this mutation causes Carney complex.<sup>21</sup> My results clearly demonstrate that DA7 and Carney complex are two unrelated disorders. DA7 patients do not have Carney complex findings, and the p.R674Q mutation is not the cause of Carney complex.

Chapter 4 starts with the description of a new syndrome. We have described this condition in a large Utah/Idaho family. Affected individuals have **camptodactyly**, **tall stature**, and **bilateral sensorineural hearing loss**; hence we named this condition the CATSHL syndrome. Other findings observed in this family include kyphoscoliosis, microcephaly, and varying degrees of mental retardation. Originally this condition was regarded as a new DA syndrome based on the similarity of limb contractures to other DA syndromes. However, following detailed clinical analyses it seems more appropriate to classify this condition as a skeletal dysplasia rather than a DA.

This condition was mapped to the short arm of chromosome 4 before I took over the project. Among the genes in the linked region, I decided to screen the coding region of *FGFR3*, based on the similarities of the findings in this family to *Fgfr3*-null mice.<sup>23,24</sup> Furthermore, activating mutations of *FGFR3* cause short stature syndromes such as achondroplasia and hypochondroplasia.<sup>25</sup> Based on homology modeling and effects of similar mutations in other receptor tyrosine kinases,<sup>26,27</sup> I suggest the p.R621H mutation I found in all affected individuals of this family causes decreased activation of FGFR3 by affecting the kinase activity of the receptor.

Since the hypothesis that DAs are caused by defects of the contractile apparatus in skeletal muscles was confirmed for three of the DAs I worked with, I tested the same hypothesis for DA5. DA5 involves the extraocular muscles, and *MYH2* and *MYH13* are both expressed in extraocular muscles,<sup>20</sup> so I chose these genes as candidates. I had access to DNA samples from eight families. I found a missense mutation in *MYH2* in one patient, causing the substitution of a conserved valine residue with isoleucine (p.V970I, Appendix A). In another family, the affected father and son had a p.R1718C

mutation in *MYH2* as well as a p.G763S mutation in *MYH13* (Appendix A). It is not clear at the moment if any of these genes is “the DA5” gene or not. However, both genes might be at least modifiers of the phenotype, and there might be other determinants of DA5. DA5 is transmitted as an autosomal dominant disorder, rather than in a complex inheritance pattern. It will therefore be worthwhile to follow up on this project since it might lead to the discovery of modifier genes and a new disease mechanism.

The revised classification of DAs left room for new designations and subtypes to be filled as novel conditions are discovered. One such condition affecting the plantar tendons, hips and elbows has been described recently.<sup>28</sup> This condition is transmitted in an autosomal dominant fashion, and the affected individuals are of normal intelligence. We proposed that this condition should be classified as DA10 (Appendix B). I conducted a genome-wide linkage analysis using STR markers and found that the condition is linked to a 45 Mb region on chromosome 2 with a maximum LOD score of 3.96 ( $\theta=0.000$ ) with the marker D2S364 (Appendix B). Among the more than 50 genes within this region, I chose the genes encoding myosin light chain 1 (*MLY1*), myosin IIIB (*MYO3B*), and caspase 10 (*CASP10*) as potential candidate genes based on their expression patterns and functions. I sequenced the entire coding regions of these genes but did not find a disease-causing mutation. It is possible that this condition might be caused by deletions or duplications, or by a mutation in the noncoding (intronic or regulatory) regions of one of the genes I screened. However, a mutation of another gene in this region is also a possibility.

In summary, the gene identification stage is completed for DA2A, DA7 and CATSHL syndrome (Table 1.2). The next step for these disorders would be characterization of the effects of the normal and mutant alleles of the responsible genes. This includes establishing detailed spatiotemporal expression patterns; gene-gene, gene-protein, and protein-protein interactions; running biochemical assays on allelic series; identifying regulatory mechanisms; and trying to recapitulate these phenotypes in animal models. Similar experiments are needed to further understand the etiopathogenesis of DA2B and DA5. However, since mutations affecting contractile proteins account for only a portion of the individuals affected with these conditions, gene identification studies and possibly further characterization of the phenotype should be conducted in parallel. Finally, the critical interval for DA10 needs to be further narrowed down. This might be possible through genotyping additional family members or by analyzing similar cases. If this is not feasible, SNP-haplotyping might be another approach. Alternatively, through a functional and positional candidate gene approach, more genes in that region can be sequenced.

The findings of this research demonstrate that defects of the contractile apparatus in skeletal muscles cause congenital contracture syndromes. This suggests that other DA syndromes might also be caused by defects of other sarcomeric proteins. Hence, gene identification studies should be conducted in carefully classified samples of other DA syndromes.

Table 1.2. The revised and extended classification of distal arthrogyposes.

Name	Known genes	Ref.
DA1	Tropomyosin 2 ( <i>TPM2</i> )	18
DA2A	Embryonic myosin heavy chain ( <i>MYH3</i> )	this work
DA2B	Troponin I2 ( <i>TNNI2</i> )	18
	Troponin T3 ( <i>TNNT3</i> )	19
	Embryonic myosin heavy chain ( <i>MYH3</i> )	this work
DA3	-	
DA4	-	
DA5	Adult skeletal myosin heavy chain 2 ( <i>MYH2</i> )	this work
	Extraocular myosin heavy chain ( <i>MYH13</i> )	this work
DA6	-	
DA7	Perinatal myosin heavy chain ( <i>MYH8</i> )	21, this work
DA8	-	
DA9	Fibrillin 2 ( <i>FBN2</i> )	17
DA10	-	
CATSHL	Fibroblast growth factor receptor 3 ( <i>FGFR3</i> )	this work

The main contribution of this research is to benefit affected individuals and their families. First, a careful clinical description is vital for better diagnosis, which leads to effective management strategies. In addition, the extensive classification facilitates gene identification. Second, molecular testing can now be offered to affected individuals and their at-risk relatives. Third, through a better understanding of normal and abnormal development, effective strategies for prevention and treatment of congenital limb malformations can be developed.

This research created more questions than it answered. From a clinician's perspective, phenotypic variability observed in patients with mutations of the same gene remains unexplained. Also, the genetic heterogeneity observed in DA2B and DA5 needs to be explored. The role of FGF signaling in muscle and tendon development and differentiation is emerging and might provide insights into normal and abnormal development of these tissues. On the other hand, the spatiotemporal expression patterns and interactions of the proteins mutated in these patients are yet to be determined. As new families are reported and additional data become available, more disease genes or previously unknown functions of some genes will be discovered.

## References

1. Christianson A, Howson CP, Modell B (2006) March of Dimes Global Report on Birth Defects: The Hidden Toll of Dying and Disabled Children. March of Dimes Birth Defects Foundation, White Plains, NY.
2. Ferretti P and Tickle C (1997) The limbs. In Embryos, Genes and Birth Defects. Ed: Thorogood P. John Wiley and Sons Ltd. p.101-132.
3. Bamshad M, Jorde LB & Carey JC (1996) A revised and extended classification of the distal arthrogyposes. *American Journal of Medical Genetics* 65:277-281.
4. Lundblom A (1932) On congenital ulnar deviation of the fingers of familial occurrence. *Acta Orthopaedica Scandinavica* 8:503-508.
5. Hall JG, Reed SD, Greene G (1982) The distal arthrogyposes: Delineation of new entities - Review and nosologic discussion. *American Journal of Medical Genetics* 11:185-239.
6. Freeman EA, Sheldon JH (1938) Cranio-carpotarsal dystrophy: undescribed congenital malformation. *Archives of Disease in Childhood* 13:277-283.
7. Krakowiak PA, Bohnsack JF, Carey JC, Bamshad M (1998) Clinical analysis of a variant of Freeman-Sheldon syndrome (DA2B). *American Journal of Medical Genetics* 76:93-98.
8. Moldenhauer E (1964) Zur klinik des Nielson-syndroms. *Dermatologische Wochenschrift* 49:594-601. Cited in Hall JG, Reed SD, Greene G (1982) The distal arthrogyposes: Delineation of new entities - Review and nosologic discussion. *American Journal of Medical Genetics* 11:185-239.
9. Gordon H, Davies D, Berman MM (1969) Camptodactyly, cleft palate and club foot: syndrome showing the autosomal-dominant pattern of inheritance. *Journal of Medical Genetics* 6:266-274.
10. Baraitser M (1982) A new camptodactyly syndrome. *Journal of Medical Genetics* 19:40-43.
11. Altman HS, Davidson HT (1939) Amyoplasia congenita (arthrogyposes multiplex congenita) *Journal of Pediatrics* 15:551-557.
12. Stewart JM, Bergstrom L (1971) Familial hand abnormality and sensori-neural deafness: A new syndrome. *Journal of Pediatrics* 78:102-110.
13. Hecht F, Beals RK. 1969. Inability to open the mouth fully: An autosomal dominant phenotype with facultative camptodactyly and short stature. In: Bergsma D, ed. Birth

Defects: Original Article Series. Part III: Limb Malformations. Vol. V. New York: Alan R Liss for The National Foundation-March of Dimes, p.96-98.

14. Wilson RV, Gaines DL, Brooks A, Carter TS, Nance WE. 1969. Autosomal dominant inheritance of shortening of the flexor profundus muscle-tendon unit with limitation of jaw excursion. In: Bergsma D, ed. Birth Defects: Original Article Series. Part III: Limb Malformations. Vol. V. New York: Alan R Liss for The National Foundation-March of Dimes, p.99-102.
15. Kawira EL, Bender HA (1985) An unusual distal arthrogryposis. American Journal of Medical Genetics 20:425-429.
16. Beals RK, Hecht F (1971) Congenital contractural arachnodactyly: A heritable disorder of connective tissue. The Journal of Bone and Joint Surgery 53A:987-993.
17. Putnam EA, Zhang H, Ramirez F, Milewicz DM (1995) Fibrillin-2 (*FBN2*) mutations result in the Marfan-like disorder, congenital contractural arachnodactyly. Nature Genetics 11:456-458.
18. Dietz HC, Cutting GR, Pyeritz RE, Maslen CL, Sakai LY, Corson GM, Puffenberger EG, Hamosh A, Nanthakumar EJ, Curristin SM, Stetten G, Meyers DA, Francomano CA (1991) Marfan syndrome caused by a recurrent de novo missense mutation in the fibrillin gene. Nature 352:337-339.
18. Sung SS, Brassington AME, Grannatt K, Rutherford A, Whitby FG, Krakowiak PA, Jorde LB, Carey JC, Bamshad M (2003) Mutations in genes encoding fast-twitch contractile proteins cause distal arthrogryposis syndromes. American Journal of Human Genetics 72:681-690.
19. Sung SS, Brassington AME, Krakowiak PA, Carey JC, Jorde LB, Bamshad M (2003) Mutations in *TNNT3* cause multiple congenital contractures: a second locus for distal arthrogryposis type 2B. American Journal of Human Genetics 73:212-214.
20. Weiss A, Leinwand LA (1996) The mammalian myosin heavy chain gene family. Annual Review of Cell and Developmental Biology 12:417-39.
21. Veugelers M, Bressan M, McDermott DA, Weremowicz S, Morton CC, Mabry CC, Lefaivre JF, Zunamon A, Destree A, Chaudron JM, Basson CT (2004) Mutation of perinatal myosin heavy chain associated with a Carney complex variant. New England Journal of Medicine 351:460-469.
22. Stratakis C, Kirschner LS, Carney JA (2001) Clinical and molecular features of the Carney complex: diagnostic criteria and recommendations for patient evaluation. The Journal of Clinical Endocrinology and Metabolism 86:4041-6.



23. Deng C, Wynshaw-Boris A, Zhou F, Kuo A, Leder P (1996) Fibroblast growth factor receptor 3 is a negative regulator of bone growth. *Cell* 84:911-921.
24. Colvin JS, Bohne BA, Harding GW, McEwen DG, Ornitz DM (1996) Skeletal overgrowth and deafness in mice lacking fibroblast growth factor receptor 3. *Nature Genetics* 12:390-397.
25. Wilkie AOM, Patey SJ, Kan SH, van den Ouweland AMW, Hamel BCJ (2002) FGFs, their receptors, and human limb malformations: clinical and molecular correlations. *American Journal of Medical Genetics* 112:266-278.
26. Ablooglu AJ, Frankel M, Rusinova E, Alexander Ross JB, Kohanski RA (2001) Multiple activation loop conformations and their regulatory properties in the insulin receptor's kinase domain. *Journal of Biological Chemistry* 275:46933-46940.
27. Williams DM, Wang D, Cole PA (2000) Chemical rescue of a mutant protein-tyrosine kinase. *Journal of Biological Chemistry* 275:38127-38130.
28. Stevenson DA, Swoboda KJ, Sanders RK, Bamshad M (2006) A new distal arthrogryposis syndrome characterized by plantar flexion contractures. *American Journal of Medical Genetics* 140A:2797-2801.

## CHAPTER 2

### MUTATIONS IN EMBRYONIC MYOSIN HEAVY CHAIN (*MYH3*) CAUSE FREEMAN-SHELDON SYNDROME AND SHELDON-HALL SYNDROME

The following chapter is a manuscript coauthored by myself, Ann Rutherford, Frank G. Whitby, Lynn B. Jorde, John C. Carey, and Michael J. Bamshad. This article is published in *Nature Genetics* in 2006 (volume 38, number 5, pages 561-565). It is presented here with the permission of the coauthors and the publisher.

## Mutations in embryonic myosin heavy chain (*MYH3*) cause Freeman-Sheldon syndrome and Sheldon-Hall syndrome

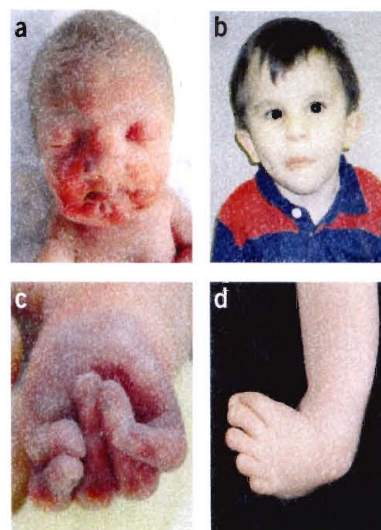
Reha M Toydemir<sup>1</sup>, Ann Rutherford<sup>2</sup>, Frank G Whitby<sup>3</sup>, Lynn B Jorde<sup>1</sup>, John C Carey<sup>2</sup> & Michael J Bamshad<sup>4</sup>

**The genetic basis of most conditions characterized by congenital contractures is largely unknown. Here we show that mutations in the embryonic myosin heavy chain (*MYH3*) gene cause Freeman-Sheldon syndrome (FSS), one of the most severe multiple congenital contracture (that is, arthrogryposis) syndromes, and nearly one-third of all cases of Sheldon-Hall syndrome (SHS), the most common distal arthrogryposis. FSS and SHS mutations affect different myosin residues, demonstrating that *MYH3* genotype is predictive of phenotype. A structure-function analysis shows that nearly all of the *MYH3* mutations are predicted to interfere with myosin's catalytic activity. These results add to the growing body of evidence showing that congenital contractures are a shared outcome of prenatal defects in myofiber force production. Elucidation of the genetic basis of these syndromes redefines congenital contractures as unique defects of the sarcomere and provides insights about what has heretofore been a poorly understood group of disorders.**

Congenital contractures in children can be divided roughly into two categories, isolated congenital contractures (such as clubfoot) and multiple congenital contractures (that is, arthrogryposis). About 1 in 3,000 children is born with arthrogryposis, and although these cases are often sporadic, children with arthrogryposis are frequently found to have an underlying syndrome that is transmitted in a mendelian pattern<sup>1-4</sup>. The most common inherited arthrogryposis

syndromes primarily affect the joints of the hands and feet, causing camptodactyly and clubfeet (Fig. 1), and are therefore known as distal arthrogryposes. To date, ten different distal arthrogryposis syndromes have been characterized<sup>2</sup>.

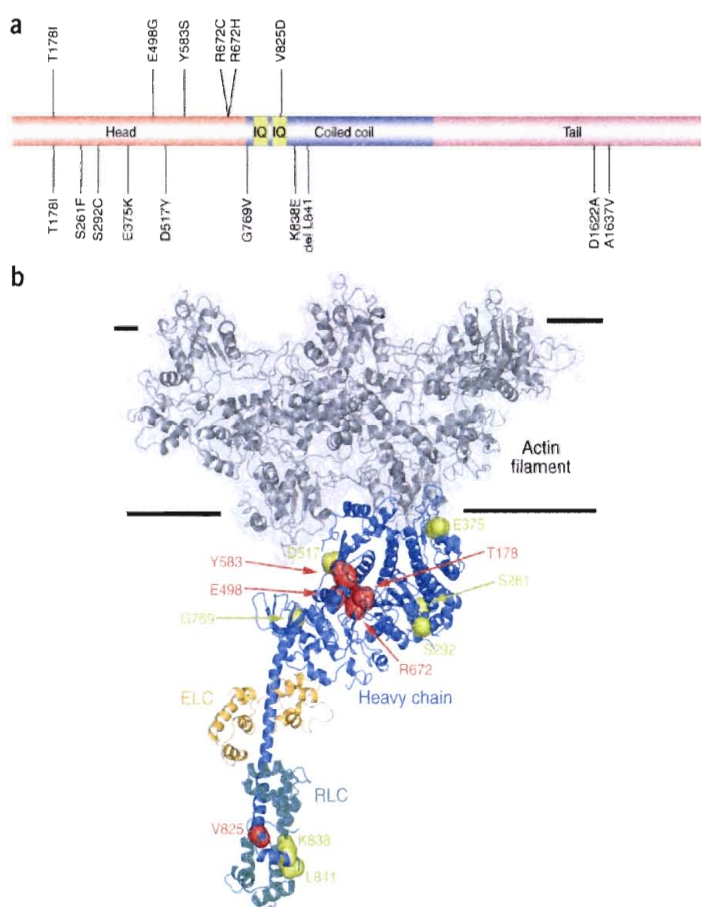
FSS is the most severe of the distal arthrogryposes and is relatively well known among clinicians because affected children also have striking contractures of the orofacial muscles (Fig. 1a)<sup>5,6</sup>. These contractures result in down-slanting palpebral fissures, prominent nasolabial folds, 'H-shaped' dimpling of the chin, pinched lips and a very small oral orifice that is often only a few millimeters in diameter at birth. Hence, FSS is also known as 'whistling face syndrome'<sup>7</sup>. The facial contractures of FSS are similar to, albeit more dramatic than, those found in children with Sheldon-Hall syndrome (SHS), the most common of the distal arthrogryposis syndromes (Fig. 1b). Accordingly, it is often difficult, particularly in children, to distinguish



**Figure 1** Clinical characteristics of FSS and SHS. (a) Children with FSS have severe contractures of the face resulting in a very small mouth, pinched lips and H-shaped dimpling of the chin. (b) In contrast, children with SHS have milder facial contractures that result in deep nasolabial folds but do not cause pinched lips or dimpling of the chin. Children with FSS and SHS have similar contractures of the hands (c) and feet (d). However, calcaneovalgus defects are often present in children with SHS but not FSS. In addition, children with FSS frequently develop scoliosis, whereas scoliosis is rare in SHS. Images in b and d are reprinted from ref. 8 with permission from the publisher, the American Academy of Pediatrics.

<sup>1</sup>Departments of Human Genetics, <sup>2</sup>Pediatrics and <sup>3</sup>Biochemistry, University of Utah, Salt Lake City, Utah, USA. <sup>4</sup>Departments of Pediatrics and Genome Sciences, University of Washington, Seattle, Washington, USA. Correspondence should be addressed to M.J.B. (mbamshad@u.washington.edu).

Received 20 December 2005; accepted 8 March 2006; published online 16 April 2006; doi:10.1038/ng1775



**Figure 2** The spectrum of *MYH3* mutations in Freeman-Sheldon syndrome (FSS) and Sheldon-Hall syndrome (SHS). (a) Schematic illustration of the embryonic myosin molecule showing head, IQ, coiled coil and tail domains. Mutations causing FSS (above) and SHS (below) localize mainly to the head domain. (b) An atomic model of the actin-myosin complex. A model of a short stretch of F-actin comprising five actin monomers is shown as a dark gray ribbon diagram surrounded by a semitransparent surface. Myosin heavy chain, essential light chain (ELC) and regulatory light chain (RLC) are shown as blue, orange and green ribbons, respectively. Distal arthrogyposis mutations are shown with oversized space-filling atoms, drawn at twice normal scale for emphasis, with a 2-Å atomic radius. FSS mutations are colored red and SHS mutations yellow. FSS mutations R672, E498, Y583 and T178 are largely buried residues that are predicted to participate in formation of the nucleotide binding site in the 50-kDa fragment groove. SHS mutations lying on the catalytic domain of the heavy chain are largely exposed to the surface but are not predicted to participate in direct actin-myosin interactions. FSS mutation V825D and SHS mutations K838E and del L841 are predicted to alter association with the RLC. T178 is colored red but was identified as both an FSS and SHS mutation.

between FSS and SHS. However, an accurate diagnosis is important because the natural history of FSS and SHS differ substantially, with FSS patients at much higher risk for strabismus, scoliosis and long-term physical disabilities<sup>8</sup>.

Several years ago, we discovered that some individuals with SHS have mutations in either *TNNI2* or *TNNT3*, which encode isoforms of troponin I and troponin T, respectively<sup>9,10</sup>. These proteins are expressed mainly in fast-twitch myofibers and are part of the multimeric troponin-tropomyosin complex of the sarcomere or contractile apparatus of myofibers. No mutations in *TNNI2* or *TNNT3* were found in individuals with FSS<sup>9</sup>. However, on the basis of these results and the phenotypic overlap among distal arthrogyposis syndromes, we hypothesized that distal arthrogyposes are, in general, caused by mutations that perturb development and/or function of the sarcomere, resulting in diminished fetal movement and contractures.

To investigate whether FSS is caused by mutations in one or more genes that encode contractile proteins, we screened 28 FSS probands (seven familial and 21 sporadic) for mutations in genes that encode myosin heavy chains (*MYH*), giving priority to genes expressed during fetal and/or perinatal development (such as *MYH1*, *MYH3*, *MYH4* and *MYH8*). In 20/28 (~72%) of FSS cases, we found a missense mutation in *MYH3* predicted to cause substitution of Arg672 with either cysteine (2083C→T;  $n = 8$ ) or histidine (2084G→A;

$n = 12$ ; Fig. 2a and Table 1). *MYH3* encodes the embryonic myosin heavy chain, and the Arg672 residue is highly conserved in all human myosins and homologs of *MYH3* studied to date (Supplementary Fig. 1 online).

In the six familial cases of FSS with an Arg672 substitution (that is, 6/20), the mutated allele segregated only with affected individuals (data not shown), and the substitution of Arg672 was confirmed to have arisen *de novo* in 10/14 sporadic cases in which parental DNA was available for analysis (Table 1). We did not find either mutation in 300 chromosomes from unrelated individuals of similar geographic ancestry. Sequencing of the remaining *MYH3* exons in these cases uncovered only silent and presumably nonpathogenic variants. Furthermore, the Arg672 residue of embryonic myosin heavy chain is paralogous to Arg674 of the perinatal myosin heavy chain that is encoded by *MYH8*. Substitution of a glutamine at Arg674 of *MYH8* was recently found to cause a distal arthrogyposis syndrome called trismus-pseudocamptodactyly (ref. 11 and R.M.T. and M.J.B., unpublished data). Like FSS, trismus-pseudocamptodactyly is characterized by contractures of the facial muscles, although the mouth is of normal size. These results show that substitution of Arg672 in the embryonic myosin heavy chain causes FSS. Additionally, genotypic data from five microsatellites bracketing *MYH3* (data not shown) showed that no unrelated, affected individuals shared a mutant *MYH3* haplotype, suggesting that the GC dinucleotide of *MYH3* at nucleotide positions 2083–2084 is a mutational hotspot.

Of the eight remaining FSS cases without an Arg672 substitution, three probands were found to have private *de novo* (E498G, Y583S) or familial (V825D) missense mutations in *MYH3* also predicted to cause substitution of highly conserved amino acids (Fig. 2a, Table 1 and

**Table 1** *MYH3* mutations in Freeman-Sheldon syndrome (FSS) and Sheldon-Hall syndrome (SHS)

Nucleotide change	Exon	Familial	Sporadic		Amino acid change	Predicted effect
			( <i>de novo</i> cases)	Total		
<b>FSS</b>						
602C→T	5		3 (3)	3	T178I	ATP binding <sup>a</sup>
1562A→G	14		1 (1)	1	E498G	Stabilization <sup>b</sup>
1817A→C	15		1 (1)	1	Y583S	ATP binding <sup>a</sup>
2083C→T	17	5	3 (3)	8	R672C	ATP binding <sup>a</sup>
2084G→A	17	1	11 (7)	12	R672H	ATP binding <sup>a</sup>
2543T→A	21	1		1	V825D	RLC interaction <sup>c</sup>
Number of mutations		7	19 (15)	26		
Number of cases studied				28		
<b>SHS</b>						
602C→T	5		2 (2)	2	T178I	ATP binding <sup>a</sup>
851C→T	8		1 (1)	1	S261F	Stabilization <sup>d</sup>
944C→G	9	1		1	S292C	Stabilization <sup>e</sup>
1192G→A	11	1		1	E375K	Actin interaction <sup>f</sup>
1618G→T	14		1	1	D517Y	Stabilization <sup>g</sup>
2375G→T	20		1	1	G769V	Stabilization <sup>h</sup>
2581A→G	21		1 (1)	1	K838E	RLC interaction <sup>c</sup>
2590_2592delCTC	21	1	1	2	del L841	RLC interaction <sup>c</sup>
4934A→C	33	1		1	D1622A	Filament formation
4979C→T	33	1		1	A1637V	Filament formation
Number of mutations		5	7 (4)	12		
Number of cases studied				38		

<sup>a</sup>–<sup>h</sup>See **Supplementary Note** online for details.

**Supplementary Fig. 1**). Three sporadic cases shared a *de novo* 602C→T mutation predicted to result in either a splicing defect or substitution of isoleucine for threonine at amino acid residue 178 (**Fig. 2a** and **Table 1**). However, sequencing of *MYH3* cDNA from lymphoblasts confirmed that splicing is normal. We did not find any of these mutations in 300 chromosomes from unrelated individuals of similar geographic ancestry.

In two individuals with prototypic features of FSS, we did not identify any pathogenic *MYH3* mutation. In these cases, the pathogenic mutation might be located in a noncoding or regulatory region of *MYH3*, or FSS could be caused by an undetected *MYH3* deletion. FSS might also be genetically heterogeneous. Although none of these explanations can be excluded, the first two possibilities are more likely, as there is no direct evidence of locus heterogeneity in FSS (such as linkage to another region). Overall, mutations in the coding region of *MYH3* account for 26/28 (93%) of FSS cases studied herein.

All of the *MYH3* mutations (R672H, R672C, E498G, Y583S and T178I) that cause FSS, except V825D, lie close to a groove that is a prominent feature of the myosin head (**Fig. 2b**). This groove lies between two parts of the large 50-kDa domain that forms the ATP binding site. Examination of the crystal structure of myosin suggests that the *MYH3* mutations that cause FSS can be tolerated without serious amino acid side-chain steric clashes or disruption of critical electrostatic interactions. Therefore, these mutations are predicted not to destabilize the structure of myosin or to promote mis-folding of the protein. Instead, each of these mutations is predicted to create small, local structural changes in myosin that could affect the conformation of the nucleotide binding site or the myosin domain-domain interactions that take place surrounding the groove during catalysis (**Fig. 2b** and **Supplementary Note** online). These domains are thought to have

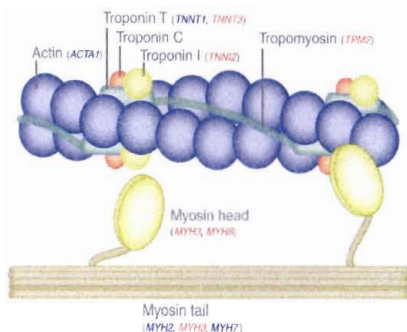
a role in ATP hydrolysis, and the groove they form has been implicated as the binding site of several myosin inhibitors<sup>12</sup>. One effect of disrupting this groove might be to perturb the catalytic activity of myosin. V825D might also change myosin's catalytic activity, albeit by a different mechanism, because it is located in a domain required for binding of calmodulin to myosin. Altering the catalytic activity of myosin might impair the ability of the sarcomere to generate normal contractile force.

Because children with FSS and SHS have similar phenotypic characteristics, we screened *MYH3* for mutations in 38 independent cases of SHS (12 familial and 26 sporadic) in whom no mutations in *TNNI2* or *TNNT3* had been found<sup>9,10</sup>. We found *MYH3* mutations in 5/12 (42%) familial and 7/26 (27%) sporadic cases, or 12/38 (~32%) of all studied cases (**Fig. 2a** and **Table 1**). Two individuals with SHS (one sporadic and one familial case) had a 3-bp deletion of *MYH3* that is predicted to encode a protein lacking Leu841, whereas all of the remaining cases had missense mutations predicted to affect highly conserved amino acid residues (**Table 1** and **Supplementary Fig. 1**). Collectively, mutations in *MYH3*, *TNNI2* and *TNNT3* account for about half of all studied cases of SHS.

None of the SHS patients had the common Arg672 substitution that causes FSS, and only one mutation (T178I) was shared between FSS and SHS cases. Nevertheless, most of the amino acid substitutions that cause SHS also localize to the head domain of myosin. However, in contrast to substitutions causing FSS, none of the amino acid residues disturbed in SHS map to the groove near the ATP binding site of myosin. Instead, amino acid substitutions that cause SHS localize primarily to surfaces that we hypothesize interact with other proteins of the contractile apparatus such as actin and troponin (**Fig. 2b**). This prediction is consistent with the observation that mutations in the genes that encode actin (*ACTA1*)<sup>13,14</sup> and troponin (*TNNI2*, *TNNT3*)<sup>9,10</sup> also cause contractures. However, the contractures caused by mutations in *ACTA1* are always accompanied by weakness and hypotonia, features that exclude the diagnosis of FSS or SHS.

Two *MYH3* mutations (D1622A, A1637V) that cause SHS result in amino acid substitutions in the rod domain of myosin that might interfere with filament formation. Therefore, disruption of either the head or the rod domain of embryonic myosin can cause congenital contractures. This result is similar to the situation for *MYH7* in which mutations in either the head or the rod domain can cause cardiomyopathy<sup>15</sup>.

Mutations in *MYH3* accounted for 38/66 (~58%) of FSS and SHS cases, making *MYH3* the most common cause of heritable congenital contractures identified to date. Moreover, *MYH3* genotype was predictive of diagnosis in 33/38 (~87%) of cases (that is, two FSS and three SHS cases shared the T178I substitution). Given that individuals with FSS typically have more severe contractures than individuals with SHS, this observation suggests that there is a positive correlation between genotype and phenotype. However, phenotypic characteristics varied widely among individuals with the same mutation. For example, FSS cases with the most common *MYH3* mutation, R672H,



**Figure 3** Schematic illustration of the contractile complex of muscle. Mutations in genes that encode sarcomeric proteins can cause congenital contractures in either distal arthrogryposis syndromes (red) or myopathies (purple).

exhibited facial and limb contractures that varied from mild to severe. Therefore, the severity of contractures in individuals with *MYH3* mutations is likely to be influenced as well by genetic and/or environmental modifiers such as the expression of other myosins or the intensity of fetal movements. No phenotypic differences distinguished SHS cases with mutations in *MYH3* from those cases with mutations in *TNN2* or *TNN3*.

The mechanism by which mutations in *MYH3* cause different phenotypes is uncertain. Mutations in other myosin genes expressed in striated muscles (cardiac and skeletal muscle) have been associated with even more varied phenotypes (Fig. 3 and Supplementary Table 1 online). Most notably, mutations in *MYH7*, which encodes a myosin heavy chain expressed in all striated muscles, cause dilated<sup>15</sup> or hypertrophic<sup>16</sup> cardiomyopathy, myosin storage myopathy<sup>17</sup> and Laing-type distal myopathy<sup>18</sup>. The region of *MYH7* in which mutations cause cardiomyopathy overlaps with those regions containing mutations causing skeletal myopathies. Similar to the shared *MYH3* mutations that can cause either FSS or SHS, the mechanism by which *MYH7* mutations cause such markedly different disorders remains to be determined.

In addition to *MYH3* and *MYH7*, mutations in *MYH2* have been reported to cause contractures in a rare condition called hereditary inclusion body myopathy<sup>19</sup>. However, mutations in *MYH2*, like those in *MYH7*, also cause weakness. In contrast, the individuals that we studied with mutations in *MYH3* do not have weakness, progressive contractures or apparent histological abnormalities of skeletal muscle. *MYH3* is expressed early in fetal development, and its expression rapidly declines after birth<sup>20,21</sup>. It is possible that other myosins might be able to compensate for defects in embryonic myosin. In *Drosophila melanogaster*, substitution of embryonic myosin for adult myosin results in normal myofiber assembly, but muscle function is impaired because the basal ATPase activities of the myosins differ—fetal and adult myosins are not functionally equivalent<sup>22,23</sup>. In humans, *MYH3* expression predominates in myotubes fated to become fast myofibers and is gradually replaced by expression of other myosin genes (*MYH1*, *MYH2* and *MYH4*). We speculate that although one or more of these myosins might be able to facilitate the development of structurally normal skeletal muscle in individuals with *MYH3* mutations, the function of fetal muscles rich in fast-twitch myofibers is functionally impaired (causing increased or diminished force production). This hypothesis predicts that there is a critical period during fetal development when functional impairment of skeletal muscles leads to

contractures but causes few or no postnatal structural abnormalities or functional impairment (that is, weakness) of skeletal muscle. Further investigation will be needed to test this hypothesis.

The function of skeletal muscle depends on the production of force by the sarcomere, the fundamental unit of contraction in all muscle cells. This force is subsequently propagated to the extracellular matrix by multiple filamentous proteins that link the sarcomere to the sarcolemma. Many mutations in genes that encode proteins involved in force transmission have been shown to cause muscular dystrophies. Our findings demonstrate that defects of sarcomeric proteins are also a common cause of congenital contracture syndromes. These syndromes are unique myopathies because affected individuals show neither weakness nor postnatal muscle damage. This suggests that other sarcomeric proteins can compensate for defects of embryonic myosin. Manipulating these compensatory mechanisms might provide a new means of treating or preventing congenital contractures.

## METHODS

**Subjects.** All studies were approved by the Institutional Review Board of the University of Utah. Informed consent was obtained from all participants, and additional consent was obtained from parents to publish photos of the children shown in Figure 1. Cases were ascertained from a general genetics clinic at the University of Utah; by direct referral from clinical geneticists, orthopedists and plastic surgeons in the US, Europe and elsewhere and from the FSS Parents Support Group. Phenotypic data were collected from a self-administered questionnaire, review of medical records, phone interviews and photographs. The questionnaire was designed to solicit information about family history, prenatal history, physical characteristics, psychosocial development and medical/surgical interventions.

A referral diagnosis of FSS made by a clinical geneticist was required for inclusion. Subsequently, phenotypic data and photographs were reviewed by two of the authors (M.J.B. and J.C.C.) to determine whether referred cases met diagnostic criteria for FSS. The diagnostic criteria included the presence of two or more of the major clinical manifestations of distal arthrogryposis plus the presence of a small pinched mouth, prominent nasolabial folds and H-shaped dimpling of the chin<sup>8</sup>. Major diagnostic criteria of the upper limbs included ulnar deviation, camptodactyly, hypoplastic and/or absent flexion creases and/or overriding fingers at birth. Major diagnostic criteria of the lower limbs included talipes equinovarus, calcaneovalgus deformities, a vertical talus and/or metatarsus varus and camptodactyly. Cases not meeting these diagnostic criteria were excluded.

Diagnostic criteria for SHS included two or more of the major clinical manifestations of distal arthrogryposis plus deep nasolabial folds, a small oral opening, webbing of the neck and a small but protuberant chin. In contrast to individuals with classical FSS, patients with SHS have a larger oral opening and lack an H-shaped dimpling of the chin.

**Mutation analysis.** We extracted genomic DNA using standard protocols. We amplified each exon of *MYH3* using HotStarTaq DNA polymerase (Qiagen) following manufacturer's recommendations and using primers previously reported<sup>11</sup>. We purified PCR products by treatment with exonuclease I (New England Biolabs) and shrimp alkaline phosphatase (USB), and we sequenced products using the dideoxy terminator method on an automatic sequencer (ABI 3100). The electropherograms of both forward and reverse strands were manually reviewed using Sequencher version 4.1 (Gene Codes).

We confirmed the presence of each mutation in each affected individual by restriction digestion performed according to the manufacturer's instructions (New England Biolabs; Supplementary Fig. 2 online). When necessary, we created a restriction enzyme recognition site by targeted mutagenesis. The primer sequences used to create such restriction sites are listed in Supplementary Table 2 online. We also used these restriction digests to screen for the presence of each putative mutation in a set of 300 chromosomes from unaffected individuals matched for geographic ancestry.

In order to analyze if the 602C→T mutation affects splicing, we isolated total RNA from the lymphoblast culture of an individual with the 602C→T

mutation using the RNeasy Protect Kit (Qiagen) and synthesized cDNA with Omniscript RT Kit (Qiagen) following the manufacturer's recommendations. We also synthesized cDNA using as a template RNA from an individual with the R672H substitution (2084G→A) as a positive control. We performed the cDNA amplification using the primers listed in **Supplementary Table 2**.

**Structural analysis.** We obtained the atomic coordinates of the X-ray crystal structure of chicken skeletal muscle myosin (Protein Data Bank), which consists of a model of the myosin subfragment-1 proteolytic fragment, with carbon-alpha coordinates only for the myosin light chains<sup>24,25</sup>. The *Gallus gallus* myosin amino acid sequence is nearly identical to that of human myosin, and all amino acid residue numbers described here refer to the human sequence. We generated full atom models of the myosin light chains with the program MAXSPROUT<sup>26</sup> and aligned atomic coordinates using the molecular graphics program O<sup>27</sup>. Atomic coordinates of F-actin were a gift of K. Holmes (Max Planck Institut Für Medizinische Forschung) and are based on a model of the thin filament described previously<sup>28</sup>. An atomic model of the actin-myosin complex was a gift of R. Milligan (The Scripps Research Institute)<sup>24</sup>. We generated figures using the molecular graphics program PyMOL<sup>29</sup>.

**URLs.** Online Mendelian Inheritance in Man is found at <http://www.ncbi.nlm.nih.gov/omim>. The Ensembl Genome Browser website is <http://www.ensembl.org>. The Protein Data Bank is found at <http://www.rcsb.org>. The PyMOL Molecular Graphics System is available at <http://www.pymol.org>.

**Accession codes.** Ensembl: *MYH1*, ENSG00000109061; *MYH3*, ENSG00000109063; *MYH4*, ENSG00000141048; *MYH5*, ENSG00000133020; *MYH13*, ENSG00000006788; OMIM: FSS, 193700; SHS, 601680; trismus-pseudocamptodactyly, 158300; dilated cardiomyopathy, 115200; hypertrophic cardiomyopathy, 192600; myosin-storage myopathy, 608358; Laing-type distal myopathy, 160500; hereditary inclusion body myopathy, 605637. Protein Data Bank: chicken skeletal muscle myosin, 2MYS.

*Note: Supplementary information is available on the Nature Genetics website.*

#### ACKNOWLEDGMENTS

We thank the families for their participation, generosity and patience, and all of the clinicians who referred study subjects. In particular, we thank the Freeman-Sheldon Parents Support Group for their cooperation; B. Kramer, S. Watkins, H. Escobar and C. Dolcourt for technical assistance; and J. Hall for discussion.

#### COMPETING INTERESTS STATEMENT

The authors declare that they have no competing financial interests.

Published online at <http://www.nature.com/naturegenetics>

Reprints and permissions information is available online at <http://npg.nature.com/reprintsandpermissions/>

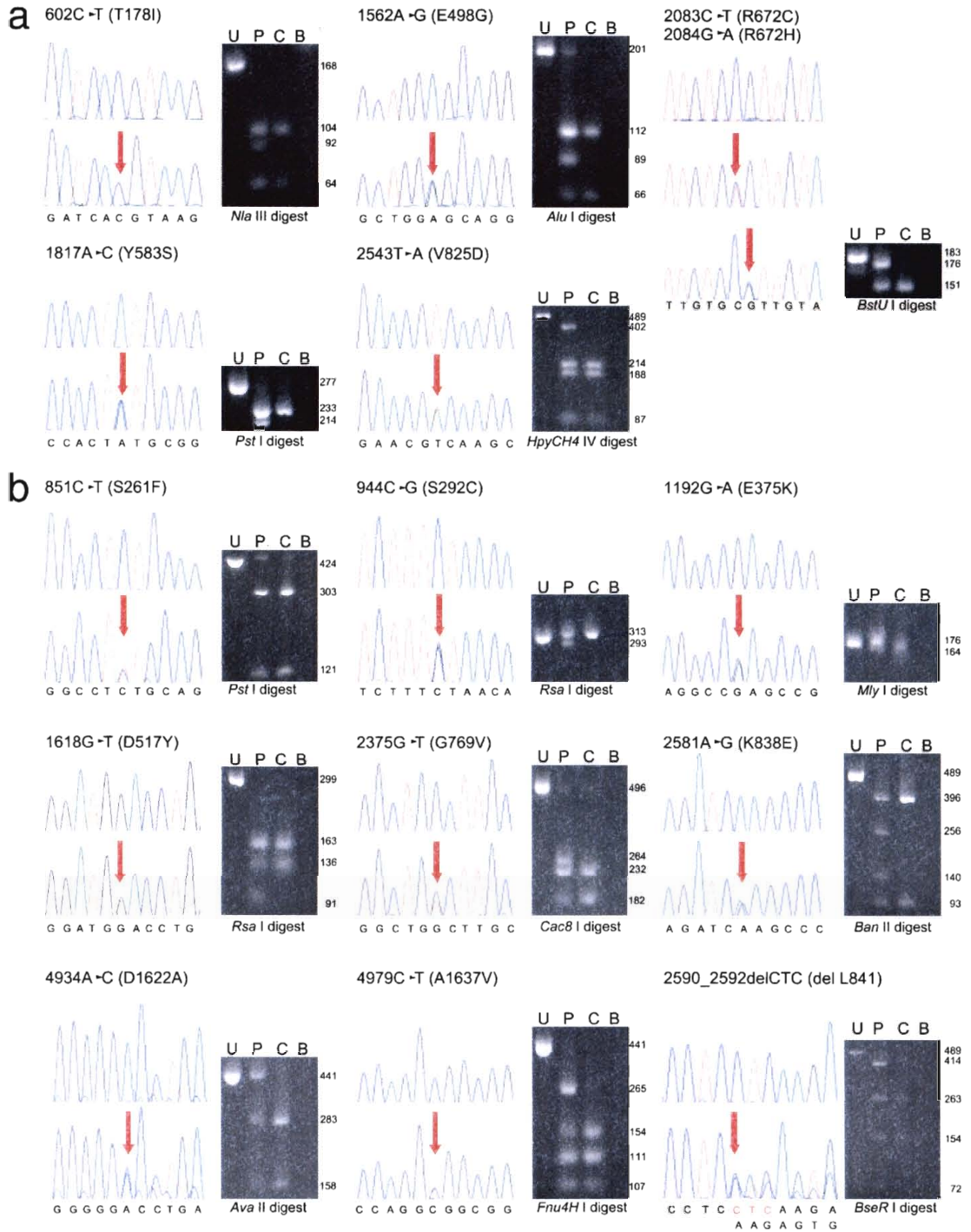
- Bamshad, M., Bohnsack, J.F., Jorde, L.B. & Carey, J.C. Distal arthrogryposis type 1: clinical analysis of a large kindred. *Am. J. Med. Genet.* **65**, 282–285 (1996).
- Bamshad, M., Jorde, L.B. & Carey, J.C. A revised and extended classification of the distal arthrogryposes. *Am. J. Med. Genet.* **65**, 277–281 (1996).
- Hall, J.G., Reed, S.C. & Greene, G. The distal arthrogryposes: delineation of new entities – review and nosologic discussion. *Am. J. Med. Genet.* **11**, 185–239 (1982).

- Krakowiak, P.A. *et al.* A variant of Freeman-Sheldon syndrome maps to 11p15.5-pter. *Am. J. Hum. Genet.* **60**, 426–432 (1997).
- Freeman, E.A. & Sheldon, J.H. Cranio-carpo-tarsal dystrophy: an undescribed congenital malformation. *Arch. Dis. Child.* **13**, 277 (1938).
- Hall, J.G. Arthrogryposes. in *Principles and Practice of Medical Genetics* (eds. Emery, A.E.H. & Rimoin, D.L.) 989–1035 (Churchill Livingstone, Edinburgh, 1992).
- Burian, F. The “whistling face” characteristic in a compound cranio-facio-corporal syndrome. *Br. J. Plast. Surg.* **16**, 140–143 (1963).
- Stevenson, D.A. *et al.* Clinical characteristics and natural history of Freeman-Sheldon syndrome. *Pediatr.* **117**, 754–762 (2006).
- Sung, S.S. *et al.* Mutations in genes encoding fast-twitch contractile proteins cause distal arthrogryposis syndromes. *Am. J. Hum. Genet.* **72**, 681–690 (2003).
- Sung, S.S. *et al.* Mutations in TNNT3 cause multiple congenital contractures: a second locus for distal arthrogryposis type 2B. *Am. J. Hum. Genet.* **73**, 212–214 (2003).
- Veugelers, M. *et al.* Mutation of perinatal myosin heavy chain associated with a Carney complex variant. *N. Engl. J. Med.* **351**, 460–469 (2004).
- Allingham, J.S., Smith, R. & Rayment, I. The structural basis of blebbistatin inhibition and specificity for myosin II. *Nat. Struct. Mol. Biol.* **12**, 378–379 (2005).
- Wallgren-Pettersson, C. *et al.* Genotype-phenotype correlations in nemaline myopathy caused by mutations in the genes for nebulin and skeletal muscle  $\alpha$ -actin. *Neuromuscul. Disord.* **14**, 461–470 (2004).
- Agrawal, P.B. *et al.* Heterogeneity of nemaline myopathy cases with skeletal muscle  $\alpha$ -actin gene mutations. *Ann. Neurol.* **56**, 86–96 (2004).
- Seidman, J.G. & Seidman, C. The genetic basis for cardiomyopathy: from mutation identification to mechanistic paradigms. *Cell* **104**, 557–567 (2001).
- Richard, P. *et al.* Hypertrophic cardiomyopathy: distribution of disease genes, spectrum of mutations, and implications for a molecular diagnosis strategy. *Circulation* **107**, 2227–2232 (2003).
- Tajsharghi, H. *et al.* Myosin storage myopathy associated with a heterozygous missense mutation in *MYH7*. *Ann. Neurol.* **54**, 494–500 (2003).
- Meredith, C. *et al.* Mutations in the slow skeletal muscle fiber myosin heavy chain (*MYH7*) cause Laing early onset distal myopathy (MPD1). *Am. J. Hum. Genet.* **75**, 703–708 (2004).
- Martinsson, T. *et al.* Autosomal dominant myopathy: Missense mutation (Glu-706 3 Lys) in the myosin heavy chain IIa gene. *Proc. Natl. Acad. Sci. USA* **97**, 14614–14619 (2000).
- Karsch-Mizrachi, I., Travis, M., Blau, H. & Levinwald, L.A. Expression and DNA sequence analysis of a human embryonic skeletal muscle myosin heavy chain gene. *Nucleic Acids Res.* **17**, 6167–6173 (1989).
- Eller, M. *et al.* Human embryonic myosin heavy chain cDNA. Interspecies sequence conservation of the myosin rod, chromosomal locus and isoform specific transcription of the gene. *FEBS Lett.* **256**, 21–28 (1989).
- Wells, L., Edwards, K.A. & Bernstein, S.I. Myosin heavy chain isoforms regulate muscle function but not myofibril assembly. *EMBO J.* **15**, 4454–4459 (1996).
- Swank, D.M. *et al.* Alternative exon-encoded regions of *Drosophila* myosin heavy chain modulate ATPase rates and actin sliding velocity. *J. Biol. Chem.* **276**, 15117–15124 (2001).
- Rayment, I. *et al.* Structure of the actin-myosin complex and its implications for muscle contraction. *Science* **261**, 58–65 (1993).
- Rayment, I. *et al.* Three-dimensional structure of myosin subfragment-1: a molecular motor. *Science* **261**, 50–58 (1993).
- Holm, L. & Sander, C. Database algorithm for generating protein backbone and side-chain co-ordinates from a C $\alpha$  trace application to model building and detection of co-ordinate errors. *J. Mol. Biol.* **218**, 183–194 (1991).
- Jones, T.A., Zou, J.Y., Cowan, S.W. & Kjeldgaard, M. Improved methods for building protein models in electron density maps and the location of errors in these models. *Acta Crystallogr. A* **47**, 110–119 (1991).
- Lorenz, M., Poole, K., Popp, D., Rosenbaum, G. & Holmes, K. An atomic model of the unregulated thin filament obtained by X-ray fiber diffraction on oriented actin tropomyosin gels. *J. Mol. Biol.* **246**, 108–119 (1995).
- DeLano, W.L. *The PyMOL Molecular Graphics System* (DeLano Scientific, San Carlos, California, 2002).

		Thr178	Glu498	Tyr583	Arg672	Val1825						
<b>a</b>	MYH3	QSILITGESGA	HMFVLEQEEYK	FSLIH <del>X</del> AGTVD	HPHFVRCIIPN	RSFMNVKHWPPW						
	MYH1	QSILITGESGA	HMFVLEQEEYK	FSLIH <del>X</del> AGTVD	HPHFVRCIIPN	RAFMN <del>V</del> KHWPPW						
	MYH2	QSILITGESGA	HMFVLEQEEYK	FALIH <del>X</del> AGVVD	HPHFVRCIIPN	RSFMNVKHWPPW						
	MYH4	QSILITGESGA	HMFVLEQEEYK	FSLVH <del>X</del> AGTVD	HPHFVRCIIPN	RAFMN <del>V</del> KHWPPW						
	MYH6	QSILITGESGA	HMFVLEQEEYK	FSLIH <del>X</del> AGTVD	HPHFVRCIIPN	RAFMGVKNWPPW						
	MYH7	QSILITGESGA	HMFVLEQEEYK	FSLIH <del>X</del> AGTVD	HPHFVRCIIPN	RAFMGVKNWPPW						
	MYH8	QSILITGESGA	HMFVLEQEEYK	FSLIH <del>X</del> AGTVD	HPHFVRCIIPN	RAFMN <del>V</del> KHWPPW						
	MYH9	QSILITGESGA	TMFILEQEEYQ	FCIIH <del>X</del> YAGKVD	NPNFVRCIIPN	AAYLKL <del>R</del> NWQW						
	MYH10	QSILITGESGA	TMFILEQEEYQ	FCIIH <del>X</del> YAGKVD	NPNFVRCIIPN	AAYLKL <del>R</del> HWQW						
	MYH11	QSILITGESGA	TMFILEQEEYQ	FSIIH <del>X</del> YAGKVD	TPNFVRCIIPN	AAYLKL <del>R</del> NWQW						
	MYH13	QSILITGESGA	HMFVLEQEEYK	FSLVH <del>X</del> AGTVD	HPHFVRCIIPN	RSFMNVKHWPPW						
	MYH14	QSILITGESGA	TMFVLEQEEYQ	FSLVH <del>X</del> YAGKVD	NPSFVRCIIPN	AAYLKL <del>R</del> HWQW						
	human	QSILITGESGA	HMFVLEQEEYK	FSLIH <del>X</del> AGTVD	HPHFVRCIIPN	RSFMNVKHWPPW						
	mouse	QSILITGESGA	HMFVLEQEEYK	FSLVH <del>X</del> AGTVD	HPHFVRCIIPN	RAFMN <del>V</del> -----						
	rat	QSILITGESGA	HMFVLEQEEYK	FSLIH <del>X</del> AGTVD	HPHFVRCIIPN	RAFMN <del>V</del> KHWPPW						
	chimp	-----	HMFVLEQEEYK	FSLIH <del>X</del> AGTVD	HPHFVRCIIPN	RSFMNVKHWPPW						
	chicken	QSILITGESGA	HMFVLEQEEYK	FSLVH <del>X</del> AGTVD	HPHFVRCIIPN	RSFMNVKHWPPW						
	fish	-----	HMFVLEQEEYK	FSLVH <del>X</del> AGTVD	HPHFVRCIIPN	RSFMNVKHWPPW						
	frog	QSILITGESGA	HMFVLEQEEYK	FSLIH <del>X</del> AGTVD	HPHFVRCIIPN	RAFMN <del>V</del> KHWPPW						
	dog	QSILITGESGA	HMFVLEQEEYK	FSLVH <del>X</del> AGTVD	HPHFVRCIIPN	RAFMN <del>V</del> KHWPPW						
<b>b</b>		Ser261	Ser292	Glu375	Asp517	Gly769	Lys838	Leu841	Asp1622	Ala1637		
	MYH3	TGKLASADIET	FYQILSNKKPE	REEQAE <del>P</del> DGTE	IDFGMDLAACI	VFFKAGLLGTL	LFFKIK <del>P</del> LLKS	KIKP <del>L</del> LKSAET	KKMEG <del>D</del> LNIEI	HANRQAA <del>E</del> ETLK		
	MYH1	TGKLASADIET	FYQILSNKKPD	REEQAE <del>P</del> DGTE	IDFGMDLAACI	VFFKAGLLGLL	LYFKIK <del>P</del> LLKS	KIKP <del>L</del> LKSAET	KKMEG <del>D</del> LNEME	HANRMAA <del>E</del> EALR		
	MYH2	TGKLASADIET	FYQILSNKKPE	REEQAE <del>P</del> DGTE	IDFGMDLAACI	VFFKAGLLGTL	LFFKIK <del>P</del> LLKS	KIKP <del>L</del> LKSAET	KKMEG <del>D</del> LNEME	HANRMAA <del>E</del> EALR		
	MYH4	TGKLASADIET	FYQILSNKKPE	REEQAE <del>P</del> DGTE	IDFGMDLAACI	VFFKAGLLGTL	LYFKIK <del>P</del> LLKS	KIKP <del>L</del> LKSAET	KKMEG <del>D</del> LNEME	HANRQAA <del>E</del> EALR		
	MYH6	TGKLASADIET	FYQILSNK <del>P</del> PE	REEQAE <del>P</del> DGTE	IDFGMDQAACI	VFFKAGLLGLL	LYFKIK <del>P</del> LLKS	KIKP <del>L</del> LKSAET	KKMEG <del>D</del> LNEME	HANRMAA <del>E</del> EAOK		
	MYH7	TGKLASADIET	FYQILSNKKPE	REEQAE <del>P</del> DGTE	IDFGMDQAACI	VFFKAGLLGLL	LYFKIK <del>P</del> LLKS	KIKP <del>L</del> LKSAER	KKMEG <del>D</del> LNEME	HANRMAA <del>E</del> EAOK		
	MYH8	TGKLASADIET	FYQILSNKKPD	REEQAE <del>P</del> DGTE	IDFGMDLAACI	VFFKAGLLGLL	LFFKIK <del>P</del> LLKS	KIKP <del>L</del> LKSAET	KKMEG <del>D</del> LNEME	HANRMAA <del>E</del> ESLR		
	MYH9	NGYIVGANIET	FYYLLSGAGEH	NTDQASMPDNT	IDFGLDLQPCI	VFFRAGVLAHL	LFTKVK <del>P</del> LLQV	KVKP <del>L</del> LQVSRQ	KKLEM <del>D</del> LKDLE	SANKNRDEA <del>I</del> TK		
	MYH10	TGYIVGANIET	FYQLLSGAGEH	NTDQASMPENT	IDFGLDLQPCI	IFFRAGVLAHL	VFTKVK <del>P</del> LLQV	KVKP <del>L</del> LQVTRQ	KKMEI <del>D</del> LKDLE	AANKARDEVI <del>K</del>		
	MYH11	TGYIVGANIET	FYYMLAGAKEK	NTDQASMPDNT	IDFGLDLQPCI	IFFKTVLAHL	LFTKVK <del>P</del> LLQV	KVKP <del>L</del> LQVTRQ	KKLEG <del>D</del> LKDLE	SAIRGREA <del>E</del> AIK		
	MYH13	TGKLASADIET	FYQILSNKKPE	REEQAE <del>P</del> DGTE	IDFGMDLAACI	VFFKAGLLGLL	LFFKIK <del>P</del> LLKS	KIKP <del>L</del> LKSAEA	KKMEG <del>D</del> LNEME	HSNRQMA <del>E</del> ETQK		
	MYH14	AGYIVGANIET	FYQLLGAGEQ	NTDQATMPDNT	IDFGLDLQPCI	IFFRAGVLAQL	LFTKVK <del>P</del> LLQV	KVKP <del>L</del> LQVTRQ	KKLEG <del>E</del> LEELK	SAGQGKEEA <del>V</del> TK		
	human	TGKLASADIET	FYQILSNKKPE	REEQAE <del>P</del> DGTE	IDFGMDLAACI	VFFKAGLLGTL	LFFKIK <del>P</del> LLKS	KIKP <del>L</del> LKSAET	KKMEG <del>D</del> LNIEI	HANRQAA <del>E</del> ETLK		
	mouse	TGKLASADIET	FYQILSNKKPE	REEQAE <del>P</del> DGTE	IDFGMDLAACI	VFFKAGLLGTL	-----	-----	KK-----	-----		
	rat	TGKLASADIET	FYQILSNKKPE	REEQAE <del>P</del> DGTE	IDFGMDLAACI	VFFKAGLLGTL	LFFKIK <del>P</del> LLKS	KIKP <del>L</del> LKSAET	KKMEG <del>D</del> LNIEI	HANRQAA <del>E</del> ETIK		
	chimp	-----	-----	-----	IDFGMDLAACI	VFFKAGLLGTL	LFFKIK <del>P</del> LLKS	KIKP <del>L</del> LKSAET	KKMEG <del>D</del> LNIEI	HANRQAA <del>E</del> ETLK		
	chicken	TGKLASADIET	FYQVTSNKKPE	REEQAE <del>P</del> DGTE	IDFGMDLAACI	VFFKAGLLGLL	LFFKIK <del>P</del> LLKS	KIKP <del>L</del> LKSAET	KKMEG <del>D</del> LNIEI	HANRQAA <del>E</del> EAOK		
	fish	TGKLASADIET	FYQLMTGHKPE	REEQAE <del>P</del> DGTE	IDFGMDLAACI	VFFKAGLLGTL	LYFKIK <del>P</del> LLKS	KIKP <del>L</del> LKSAET	KKMEG <del>D</del> LNEME	HANRMAA <del>E</del> EAOK		
	frog	TGKLASADIET	FYQILSNKKPE	REEQAE <del>P</del> DGTE	IDFGMDLAACI	VFFKAGLLGTL	LYFKIK <del>P</del> LLRS	KIKP <del>L</del> LSAET	KKMEG <del>D</del> LNEME	HANRIAT <del>E</del> TQK		
	dog	TGKLASADIET	FYQILSNKKPE	REEQAE <del>P</del> DGTE	IDFGMDLAACI	VFFKAGLLGTL	LYFKIK <del>P</del> LLKS	KIKP <del>L</del> LKSAET	KKMEG <del>D</del> LNEME	HANRQAA <del>E</del> EATR		

**Supplementary Figure 1.** Amino acid alignments of the regions surrounding the mutated residues in FSS (a) and SHS (b) patients. The Ensembl accession codes of the paralogous sequences are: MYH3, ENSG00000109063; MYH1, ENSG00000109061; MYH2, ENSG00000125414; MYH4, ENSG00000141048; MYH6, ENSG00000197616; MYH7, ENSG00000092054; MYH8, ENSG00000133020; MYH9, ENSG00000100345; MYH10, ENSG00000133026; MYH11, ENSG00000133392; MYH13, ENSG00000006788; MYH14, ENSG00000105357; The Ensembl accession codes of the orthologous sequences are: mouse (*Mus musculus*), ENSMUSG000000057003; rat (*Rattus norvegicus*), ENSRNOG000000031497; chimp (*Pan troglodytes*), ENSPTRG000000008773; chicken (*Gallus gallus*), ENSGALG00000000965; fish (*Danio rerio*), ENSDARG00000014711; frog (*Xenopus tropicalis*), ENSXETG00000016237; dog (*Canis familiaris*), ENSCAF000000017575.





**Supplementary Figure 2.** Electropherograms and restriction digests in FSS (a) and SHS (b) families with respective controls. The missense mutations are shown with arrows, deleted nucleotides are shown in red. U: uncut PCR, P: patient, C: control, B: blank.

**Supplementary Note.** Structure-function analysis of MYH3 mutations.

<sup>a</sup> R672, Y583, and T178 sidechains point into a cavity that lies adjacent to the nucleotide binding site. Mutations of these residues are predicted to alter the active site geometry surrounding the nucleotide binding site.

<sup>b</sup> E498 forms a salt bridge interaction with R714, which provides stabilization of the subdomains. E498G mutation is expected to abolish this salt bridge, destabilizing subdomain interactions.

<sup>c</sup> V825D, K838E, and del L841 are predicted to alter regulatory light chain (RLC) interactions with the heavy chain (HC). Del L841 lies at the HC-RLC interface and deletion of this residue would likely result in extensive changes in HC-RLC interaction in the region. V825D mutation introduces a charged residue into an otherwise hydrophobic interaction, possibly destabilizing HC-RLC interaction. K838E causes a charge reversal in a region of the HC dominated by positive charge.

<sup>d</sup> S261 hydrogen bonds to residues in a loop (residues 450-458). S261F mutation disrupts this loop and causes steric clash, possibly altering stability of the large beta-sheet that forms the core of the head domain.

<sup>e</sup> S292C is an isostructural mutation that might disrupt an important hydrogen bonding interaction, perhaps altering enzyme kinetics or the stability of a state of the head domain during catalysis.

<sup>f</sup> E375K results in charge reversal at a surface-exposed loop 25 angstroms distant from the actin-myosin interface, but is not predicted to alter the conformation of the loop nor that of a neighboring loop (residues 402-418) that makes contact with actin. The effect of this mutation might alter actin-myosin interaction during a different state of the contractile process.

<sup>g</sup> D517Y neutralizes a surface charge, but is not predicted to have a large structural consequence. This mutation might affect interactions between this surface and regions of the protein that are disordered in the existing crystal structure, or perhaps affects surface interactions when myosin undergoes conformational changes during catalysis.

<sup>h</sup> G769V mutation results in greater geometric constraint of the protein backbone where this residue lies in a turn at the start of a helix. Reduced flexibility in this turn might prevent access of a required conformational state during catalysis.

**Supplementary Table 1.** Mutations reported in myosin genes expressed in striated muscles that cause inclusion body myopathy (blue), autosomal dominant myopathy (red), hypertrophic cardiomyopathy (black), atrial septal defect (light blue), dilated cardiomyopathy (pink), distal myopathy (dark blue), myosin storage myopathy (purple), hyalin body myopathy (brown), and Trismus-Pseudocamptodactyly syndrome (orange). The paralogous residues in *MYH3* are shown in parentheses. Only missense and nonsense mutations are shown. Residues mutated in <sup>(1)</sup> FSS and <sup>(2)</sup> SHS are also shown.

<i>MYH2</i>	<i>MYH7</i> (Continued)	<i>MYH7</i> (Continued)	<i>MYH7</i> (Continued)
E706K (E701)	A355T (A356)	R694H (R695)	Q882E (Q883)
V970I <sup>a</sup> (V965)	K383N (K384)	N696S (N697)	E894G (E895)
L1061V <sup>a</sup> (L1056)	A385V (A386)	R712L (R713)	E903K (E904)
	L390V (L391)	G716R (G717)	C905F (C906)
	R403L (R404)	R719P (R720)	L908V (L909)
<b><i>MYH6</i></b>		R719Q (R720)	E921K (E922)
R795Q (R794)	R403N (R404)	R719W (R720)	E924K (E925)
E849N <sup>b</sup> (I819)	R403W (R404)	R723C (R724)	E924Q (E925)
	V404L (V405)	R723G (R724)	E927K (E928)
	V404M (V405)	A728V (S729)	D928N (D929)
<b><i>MYH7</i></b>	V406M (V407)	P731L (P732)	E930K (E931)
A26V (A27)	G407V (G408)	G733E (G734)	E931K (E932)
V39M (V40)	V411I (V412)	Q734E (Q735)	E935K (E936)
R54X (S55)	A428V (S429)	I736M (I737)	E949K (E950)
V59I (V60)	A430E (S431)	I736T (I737)	D953H (D954)
Y115H (Y116)	M435T (L436)	G741A (A742)	L961R (L962)
T124I (T125)	V440M (V441)	G741R (A742)	G1057S (G1058)
R143G (R144)	I443T (I444)	G741R (A742)	L1135R (Q1136)
R143Q (R144)	K450E (K451)	G741W (A742)	E1218Q (E1219)
R143W (R144)	R453C (R454)	E743D (E744)	E1356K (E1357)
S148I (Q149)	R453H (R454)	V763G (V764)	T1377M (T1378)
Y162C (Y163)	R453L (R454)	F764I (F765)	A1379T (A1380)
N187K (N188)	N479S (N480)	G768R (G769) <sup>2</sup>	R1382W (R1383)
T188N (T189)	E483K (E484)	E774V (E775)	R1420W (R1421)
R190T (R191)	E499K (E500)	D778E (D779)	K1459N (K1460)
Y194S (Y195)	E500A (E501)	D778G (D779)	R1500P (R1501)
A196T (A197)	I511T (I512)	D778V (D779)	T1513S (T1514)
R204H (L205)	F513C (F514)	E779X (D780)	E1555K (E1556)
K207Q (K208)	M515R (M516)	S782N (A783)	A1663P (G1664)
P211L (K212)	L517M (L518)	R787H (R788)	V1691M (T1692)
Q222K (Q223)	S532P (S533)	L796F (L797)	L1706P (L1708)
A223T (A224)	G584R (G585)	A797T (M798)	R1712W <sup>c</sup> (R1713)
L227V (L228)	G584S (G585)	M822V (M823)	E1768K (E1769)
N232S (N233)	D587V (D588)	V824I (V825) <sup>1</sup>	S1776G (S1777)
F244L (F245)	L601V (L602)	E846K (E847)	A1777T (A1778)
K246Q (K247)	N602S (N603)	E846Q (E847)	R1846G (R1846)
R249Q (R252)	V606M (V607)	M852T (M853)	T1854M (R1846)
G256E (G259)	K615N (R616)	R858C (K859)	H1901L (H1902)
I263M (I264)	S642I (S643)	R869C (K870)	T1929M (S1930)
I263T (I264)	M659I (M660)	R869G (K870)	
F312C (F313)	R663C (R664)	R869H (K870)	
V320M (V321)	R663H (R664)	R870C (R871)	
A326P (A327)	R663S (R664)	R870H (R871)	
E328G (E329)	R671C (R672) <sup>1</sup>	M877K (L878)	
M349T (L350)	R694C (R695)		
K351E (K352)			

All mutations are listed in the Human Gene Mutation Database, which can be accessed at <http://www.hgmd.org> (Stenson *et al.* The Human Gene Mutation Database (HGMD®); 2003 Update. *Hum. Mutat.* **21**, 577-581 (2003)) except: <sup>(a)</sup> Tajsharghi, H. *et al.* Mutations and sequence variation in the human myosin heavy chain IIa gene (*MYH2*). *Eur. J. Hum. Genet.* **13**, 617-622 (2005); <sup>(b)</sup> Ching, Y. H. *et al.* Mutation in myosin heavy chain 6 causes atrial septal defect. *Nat. Genet.* **37**, 423-428 (2005); <sup>(c)</sup> Hougs, L. *et al.* One third of Danish hypertrophic cardiomyopathy patients with *MYH7* mutations have mutations [corrected] in *MYH7* rod region. *Eur. J. Hum. Genet.* **13**, 161-165 (2005).

**Supplementary Table 2.** PCR primers and restriction enzymes used for mutation analysis. Nucleotides incorporated to create restriction sites for mutation screening and to create control restriction sites are shown in blue and red, respectively. Oligonucleotide primers were designed to analyze if the 602C→T mutation affected splicing. The cDNA of a patient with R672H mutation (2084G→A) was also sequenced as a positive control.

Mutations	Forward Primers	Reverse Primers	Enzymes
<i>FSS Mutations</i>			
T178I	5'-TGCTCCAACACTTTCTAATGAA-3'	5'-GGGTAGAATCGGGAAGCTCT-3'	<i>Nla</i> III
G498R	5'-CCTTCCTTCTTGTACTCCTCCAGC-3'	5'-TGACAGGAACCTGGGGCAATGAG-3'	<i>Alu</i> I
Y583R	5'-CACTGTAGTCCACGGTGCCTGC-3'	5'-CCCACCGTAAAGCTCTTCTCA-3'	<i>Pst</i> I
R672C/H	5'-TACACCGCGGCTGGTGCAGA-3'	5'-AAGAACTACTCACCCCTCATTTTGCG-3'	<i>BstU</i> I
V825D	5'-ACACAAGCTGTGTGCAGAGG-3'	5'-GCAAAAATCCCCACCAATAA-3'	<i>HpyCH4</i> IV
<i>SHS Mutations</i>			
S261F	5'-CCCATAAGATGAATAGGAACTATTGG-3'	5'-AAACTTTCCTGTGACTGTAGA-3'	<i>Pst</i> I
S292C	5'-CCCATAAGATGAATAGGAACTATTGG-3'	5'-ATGAGCTCAGGCTTCTTGGTA-3'	<i>Rsa</i> I
E375K	5'-ACCTTCTGTGCCATCCGACT-3'	5'-GCCAACTGACTGACGTGCT-3'	<i>Mly</i> I
D517Y	5'-GGAATGTTGACAGTCTTTGATTC-3'	5'-TGCAGTAATGAGCAGAAGAGTC-3'	<i>Rsa</i> I
G769V	5'-GGAAGAGAGGCTGAACACTACA-3'	5'-TTTCTGAGAGAGACTCCCCTTC-3'	<i>Cac8</i> I
K838E	5'-ACACAAGCTGTGTGCAGAGG-3'	5'-GCAAAAATCCCCACCAATAA-3'	<i>Ban</i> II
del L84I	5'-ACACAAGCTGTGTGCAGAGG-3'	5'-GCAAAAATCCCCACCAATAA-3'	<i>BseR</i> I
D1622A	5'-CTGCAGGGTAGTGGAGCTG-3'	5'-GCCCAGCCTACATTCTGAG-3'	<i>Ava</i> II
A1637V	5'-CTGCAGGGTAGTGGAGCTG-3'	5'-GCCCAGCCTACATTCTGAG-3'	<i>Fnu4H</i> I
<i>Splice Site Mutation</i>			
602C→T	5'-TGATCGTGAAAACCAGTCCATTCT-3'	5'-TTGGCCAGGTCCCCAGTAGCT-3'	
2084G→A	5'-CTCTGCCCTTTTCAGGGAAAACC-3'	5'-CTGGTGCAGAACAAGGCTGTGT-3'	

## CHAPTER 3

### TRISMUS-PSEUDOCAMPTODACTYLY SYNDROME IS CAUSED BY A RECURRENT MUTATION IN *MYH8*

The following chapter is a manuscript coauthored by myself, Harold Chen, Virginia K. Proud, Hans van Bokhoven, Rick Martin, Constantine A. Stratakis, Lynn B. Jorde, and Michael J. Bamshad. This article is published in *American Journal of Medical Genetics* in 2006 (volume 140A, number 22, pages 2387-2393). It is presented here with the permission of the coauthors and the publisher.

**Rapid Publication**  
**Trismus-Pseudocamptodactyly Syndrome Is  
 Caused by Recurrent Mutation of *MYH8***

**Reha M. Toydemir,<sup>1</sup> Harold Chen,<sup>2</sup> Virginia K. Proud,<sup>3</sup> Rick Martin,<sup>4</sup> Hans van Bokhoven,<sup>5</sup>  
 Ben C. J. Hamel,<sup>5</sup> Joep H. Tuerlings,<sup>5</sup> Constantine A. Stratakis,<sup>6</sup>  
 Lynn B. Jorde,<sup>1</sup> and Michael J. Bamshad<sup>7,8\*</sup>**

<sup>1</sup>Department of Human Genetics, University of Utah, Salt Lake City, UT

<sup>2</sup>Department of Pediatrics, Division of Perinatal Genetics, Louisiana State University Health Sciences Center-Shreveport, Shreveport, LA

<sup>3</sup>Department of Pediatrics, Division of Medical Genetics, Children's Hospital of The King's Daughters, Eastern Virginia Medical School, Norfolk, VA

<sup>4</sup>Department of Pediatrics, Washington University School of Medicine, St. Louis, MO

<sup>5</sup>Department of Human Genetics, Radboud University, Nijmegen Medical Center, Nijmegen, The Netherlands

<sup>6</sup>Section on Endocrinology and Genetics, Developmental Endocrinology Branch, National Institute of Child Health and Human Development, National Institutes of Health, Bethesda, MD

<sup>7</sup>Departments of Pediatrics and Genome Sciences, University of Washington, Seattle, WA

<sup>8</sup>Children's Hospital and Regional Medical Center, Seattle, WA

Received 1 August 2006; Accepted 24 August 2006

Trismus-pseudocamptodactyly syndrome (TPS) is a rare autosomal dominant distal arthrogryposis (DA) characterized by an inability to open the mouth fully (trismus) and an unusual camptodactyly of the fingers that is apparent only upon dorsiflexion of the wrist (i.e., pseudocamptodactyly). TPS is also known as Dutch-Kentucky syndrome because a Dutch founder mutation is presumed to be the origin of TPS cases in the Southeast US, including Kentucky. To date only a single mutation, p.R674Q, in *MYH8* has been reported to cause TPS. Several individuals with this mutation also had a so-called "variant" of Carney complex, suggesting that the pathogenesis of TPS and Carney complex might be shared. We screened *MYH8* in four TPS pedigrees, including the original Dutch family in which TPS was reported. All four TPS families shared the p.R674Q substitution. However,

haplotype analysis revealed that this mutation has arisen independently in North American and European TPS pedigrees. None of the individuals with TPS studied had features of Carney complex, and p.R674Q was not found in 49 independent cases of Carney complex that were screened. Our findings show that distal arthrogryposis syndromes share a similar pathogenesis and are, in general, caused by disruption of the contractile complex of muscle.

© 2006 Wiley-Liss, Inc.

**Key words:** distal arthrogryposis; trismus-pseudocamptodactyly; Dutch-Kentucky syndrome; Hecht-Beals syndrome; myosin heavy chain; Carney complex

**How to cite this article:** Toydemir RM, Chen H, Proud VK, Martin R, van Bokhoven H, Hamel BCJ, Tuerlings JH, Stratakis CA, Jorde LB, Bamshad MJ. 2006. Trismus-pseudocamptodactyly syndrome is caused by recurrent mutation of *MYH8*. *Am J Med Genet Part A* 140A:2387–2393.

### INTRODUCTION

Trismus-pseudocamptodactyly syndrome (TPS, OMIM #158300) is a rare autosomal dominant disorder characterized by an inability to fully open the mouth (i.e., trismus) and an unusual camptodactyly of the fingers that is apparent only upon hyperextension of the wrist (i.e., pseudocamptodactyly). Additional reported features of TPS include clubfoot, shortened "hamstring" muscles, and short stature. The penetrance of TPS appears to be high,

Grant sponsor: U.S. National Institutes of Health; Grant number: R01-HD048895; Grant sponsor: U.S. Center for Disease Control; Grant sponsor: University of Utah Clinical Genetics Research Program; Grant sponsor: University of Utah Graduate Research Fellowship; Grant sponsor: National Institute of Child Health and Human Development Intramural Program.

\*Correspondence to: Michael J. Bamshad, M.D., Department of Pediatrics, Division of Genetics and Developmental Medicine, University of Washington School of Medicine, 1959 NE Pacific Street, HSB RR349, Seattle, WA 98195. E-mail: mbamshad@u.washington.edu

DOI 10.1002/ajmg.a.31495

although clinical characteristics vary widely within families, and no single feature, including either trismus or pseudocamptodactyly, is present in all affected individuals.

TPS was originally described by Hecht and Beals [1969] and Wilson et al. [1969]. Over the past 40 years, at least 20 families have been reported [De Jong, 1971; Horowitz et al., 1973; Mabry et al., 1974; Ter Haar and van Hoof, 1974; Yamashita and Arnet, 1980; Mercuri, 1981; Robertson et al., 1982; O'Brien et al., 1984; Tsukahara et al., 1985; Markus, 1986; Vaghadia and Blackstock, 1988; Chen et al., 1992; Teng et al., 1994; Karras and Wolford, 1995; Geva et al., 1997; Lano and Werkhaven, 1997; Adams and Rees, 1999; Seavello and Hammer, 1999; Lefavre and Aitchison, 2003; Pelo et al., 2003; Skinner and Rees, 2004; Carlos et al., 2005; Guimaraes and Marie, 2005]. TPS is also known by the popular label, Dutch-Kentucky syndrome because a Dutch founder was proposed to have been the common ancestor of many of the cases reported in the Southeast US [Mabry et al., 1974]. However, while most reported cases are from North America, individuals with TPS have been reported from the Netherlands, Germany, United Kingdom, Japan, Belgium, and Guatemala [Tsukahara et al., 1985; Hertrich and Schuch, 1991; Rombouts and Verellen-Dumoulin, 1992; Hirano et al., 1994; Teng et al., 1994; Nagata et al., 1999; Carlos et al., 2005].

In Bamshad et al.'s [1996] re-organization of Hall et al.'s [1982] classification of the distal arthrogryposis (DA) syndromes, 10 different DA disorders were categorized hierarchically according to their similarity with one another. TPS was labeled DA type 7 (DA7) because of its unusual hand contractures and lack of similarity to more common DAs such as DA type 1, Freeman-Sheldon syndrome (FSS or DA2A), or Sheldon-Hall syndrome (SHS or DA2B). In retrospect, greater emphasis should probably have been given to the overlapping facial characteristics of TPS with FSS and SHS since all three conditions are characterized by a small mouth, and individuals with FSS or SHS occasionally have trismus. Moreover, TPS has been reported to be caused by a single mutation in *MYH8*, a gene that encodes the perinatal myosin heavy chain [Veugelers et al., 2004], while FSS and SHS recently were reported to be caused by mutations in the gene that encodes the embryonic myosin heavy chain, *MYH3* [Toydemir et al., 2006]. Therefore, TPS, FSS, and SHS appear to have a similar molecular pathogenesis as well as overlapping clinical characteristics.

To further characterize the molecular basis of TPS and determine whether families reported from the Netherlands and Southeastern US shared a founder mutation in *MYH8*, we sequenced *MYH8* in four families with TPS and genotyped a set of microsatellites in the region bracketing *MYH8* in order to reconstruct *MYH8* haplotypes. These four TPS

families include representatives from both the original Dutch kindred (Fig. 1A) and several TPS kindreds from the Southeast US (Fig. 1B–D). Furthermore, 3 of 19 members of the TPS family in which a *MYH8* mutation was reported originally were also affected with a so-called "variant" of Carney complex, an autosomal dominant condition characterized by skin pigmentary abnormalities, myxomas, endocrine tumors or over activity, and schwannomas [Kirschner et al., 2000; Veugelers et al., 2004] that manifest with cardiac myxomas and spotty skin pigmentation. This observation prompted Veugelers et al. [2004] to conclude that the mutation in *MYH8* that caused TPS also caused Carney complex and that the pathogenesis of the two disorders might overlap. Accordingly, we also screened 49 independent cases of Carney complex to determine whether they had the mutation reported to cause TPS.

## SUBJECTS AND METHODS

All studies were approved by the Institutional Review Board of the University of Utah and the intramural program of the National Institute of Child Health and Human Development. Inclusion criteria included the presence of congenital contractures of two or more different body areas, including but not limited to pseudocamptodactyly of the fingers and trismus. If at least one affected family member met these criteria, the diagnostic criteria were relaxed for other family members such that only pseudocamptodactyly, camptodactyly, or trismus need be present to confirm the diagnosis of TPS.

Clinical descriptions of the families A and B (Fig. 1) have been published [Ter Haar and van Hoof, 1974; Chen et al., 1992]. After obtaining informed consent, genomic DNA was extracted, using standard protocols, from peripheral lymphocytes from 19 affected and 12 unaffected individuals in four TPS families (Fig. 1) and 49 individuals with Carney complex who were negative for mutations in *PRKARIA*, the only gene confirmed to date to cause Carney complex. The entire coding region of *MYH8* was PCR-amplified using previously reported primers [Veugelers et al., 2004] and HotstarTaq DNA polymerase (Qiagen, Inc., Valencia, CA) following the manufacturer's recommendations. PCR products were purified by exonuclease I (New England Biolabs, Inc., Beverly, MA) and shrimp alkaline phosphatase (USB Corp., Cleveland, OH) treatment. Purified PCR products were sequenced using the ABI BigDye Terminator v.3.1 chemistry (Applied Biosystems, Inc., Foster City, CA) and an ABI 3100 automated sequencer (Applied Biosystems, Inc.). The sequences were analyzed by the Sequencher 4.1 program (Gene Codes Corp., Ann Arbor, MI).

The presence of the c.2021G > A mutation was confirmed in each family member by restriction digestion with both *BsiWI* (New England Biolabs,

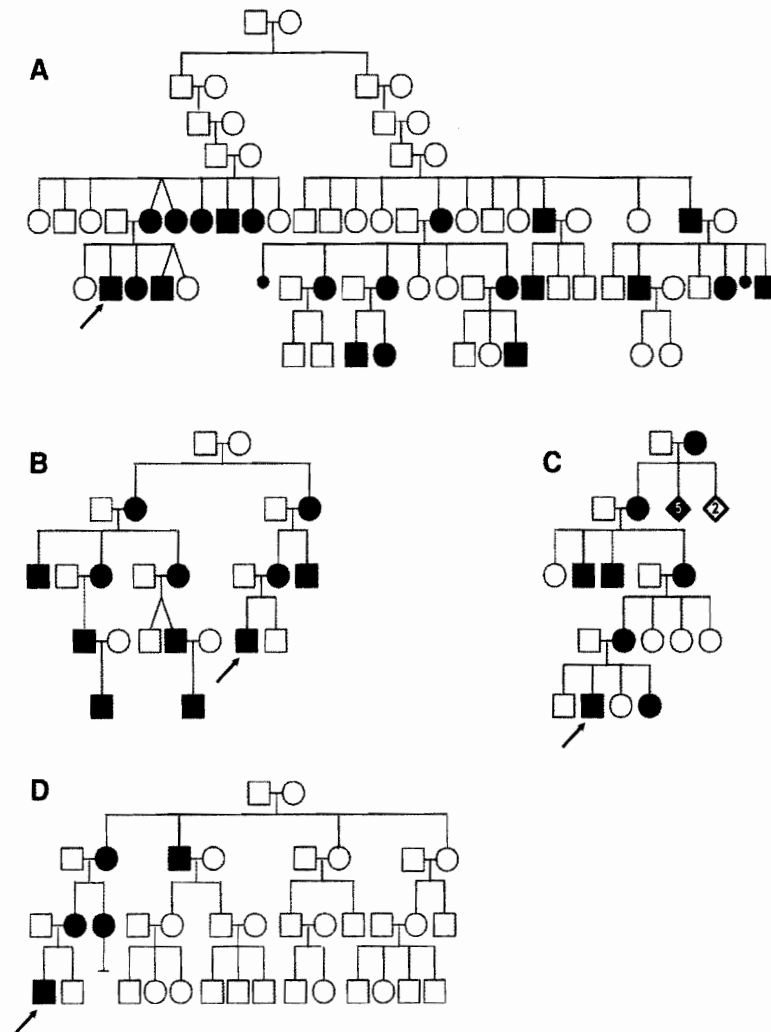


FIG. 1. Pedigrees of TPS families (A–D). Filled symbols denote affected individuals and open symbols unaffected individuals. Arrows indicate the proband

Inc.) and *TspRI* (NEB, Inc.) performed according to the manufacturers' instructions. Using these restriction enzymes, 480 chromosomes from unrelated, presumably unaffected individuals matched for geographic ancestry were also screened.

Molecular modeling was done with PyMOL [DeLano, 2002], using the chicken myosin head structure as a model [Rayment et al., 1993a,b].

## RESULTS

In each affected individual in each TPS pedigree, we identified a guanine to adenine missense mutation at nucleotide position 2021 (c.2021G > A) of *MYH8* (Fig. 2) that results in substitution of a highly conserved arginine residue with a glutamine (p.R674Q). This mutation was not observed in the

unaffected family members or in 480 control chromosomes. This mutation is identical to the mutation that was reported previously in a family with TPS and a variant of Carney complex [Veugelers et al., 2004].

To determine whether individuals from different TPS pedigrees with c.2021G > A shared this mutation as a result of a recent common ancestor or recurrent mutation, we genotyped four microsatellites (D17S1879, D17S520, D17S1852, D17S1159) spanning a 500 kb region around *MYH8* in an affected parent and an affected child from each TPS kindred. These genotypes were used to manually construct the c.2021G > A-bearing *MYH8* haplotypes segregating in each pedigree. Analysis of haplotype sharing among TPS pedigrees revealed that while each of the pedigrees ascertained in the US shared the same



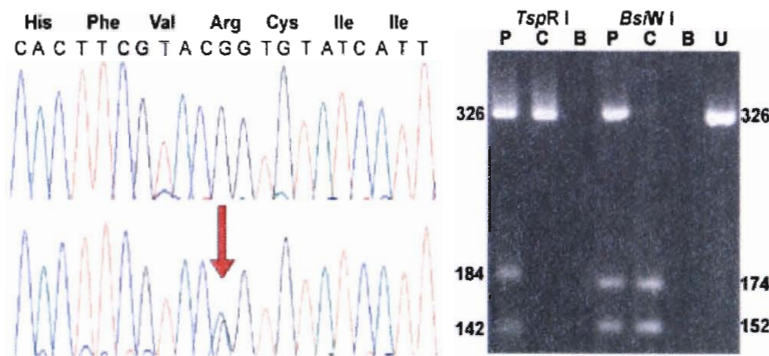


FIG. 2. The c.2021G > A mutation (red arrow) in *MYH8* causes an arginine to glutamine substitution. This mutation creates a *TspRI* site and destroys a *BstWI* site. P: patient, C: control, B: blank, U: uncut PCR product.

*MYH8* haplotype, this haplotype was not shared with the Dutch TPS kindred (Fig. 3). Therefore, the hypothesis that TPS families in the Southeast US share c.2021G > A-bearing *MYH8* haplotypes as a consequence of a recent shared Dutch ancestor with TPS is rejected.

None of the individuals studied herein with TPS were reported to have multiple hyper-pigmented macules and/or cardiac myxomas like those previously reported in several individuals with TPS caused by c.2021G > A [Veugelers et al., 2004]. The c.2021G > A mutation was not found in any of the 49 Carney complex cases that were screened, consistent with the absence of TPS stigmata in any Carney complex patient studied by an international consortium [Stratakis et al., 2004].

**DISCUSSION**

These results demonstrate that (1) all cases of TPS studied to date are caused by an identical c.2021G > A mutation in *MYH8* that causes a p.R674Q substitution; (2) c.2021G > A has arisen independently at least twice; (3) Dutch and US TPS pedigrees do not share a founder mutation; and (4) c.2021G > A might be associated with increased risk of cardiac myxomas but it rarely, if ever, causes Carney complex.

The molecular etiology of TPS has been further clarified with the characterization of four new and putatively independent TPS pedigrees. The observation that *MYH8*-c.2021G > A haplotypes are identical suggests that all of the TPS cases from North America studied to date are likely descendants of a common ancestor and therefore represent only a single founder mutation. However, *MYH8*-c.2021G > A in the Dutch TPS kindred appears to have arisen independently, indicating that c.2021G > A has arisen at least twice. Whether this is a mutational hotspot and/or whether other mutations in *MYH8* cause TPS will require testing of additional individuals with TPS, ideally those with a geographic ancestry outside of Europe.

The arginine residue affected by the c.2021G > A mutation is conserved in all known human genes that encode myosin heavy chains and homologs of *MYH8* in a variety of species (Fig. 4). This observation suggests that this arginine residue plays a critical role in the normal function of myosin heavy chain 8. Based on homology modeling, substitution of glycine for this arginine residue is not likely to cause major structural perturbation of myosin, but this arginine does lie on the surface of a groove between the two major domains of the myosin head near the ATP binding site (Fig. 5). Therefore, the c.2021G > A mutation might disrupt the catalytic activity of myosin.

To date, the only TPS cases reported with characteristics of Carney complex are those in the family reported by Veugelers et al. [2004]. None of the TPS cases studied herein had any of the features of Carney complex, nor have individuals with Carney complex accompanied by trismus and/or pseudocamptodactyly been reported [Stratakis et al., 2004]. Additionally, we did not find c.2021G > A in 49 independent cases of Carney complex, nor have other mutations in *MYH8* been reported to cause Carney complex [Stratakis et al., 2004].

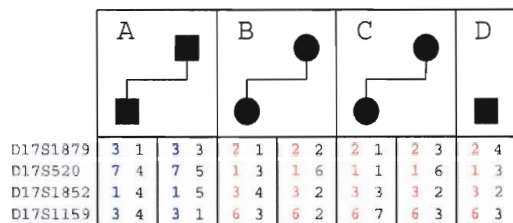


FIG. 3. p.R674Q-*MYH8* haplotypes in TPS families (A–D).

	Arg674		Arg674
<b>MYH8</b>	HPHFVRCIIPN	<b>human</b>	HPHFVRCIIPN
<b>MYH1</b>	HPHFVRCIIPN	<b>mouse</b>	HPHFVRCIIPN
<b>MYH2</b>	HPHFVRCIIPN	<b>rat</b>	HPHFVRCIIPN
<b>MYH3</b>	HPHFVRCIIPN	<b>chimp</b>	HPHFVRCIIPN
<b>MYH4</b>	HPHFVRCIIPN	<b>chicken</b>	HPHFVRCIIPN
<b>MYH6</b>	HPHFVRCIIPN	<b>fish</b>	HPHFVRCIIPN
<b>MYH7</b>	HPHFVRCIIPN	<b>frog</b>	HPHFVRCIIPN
<b>MYH9</b>	NPNFVRCIIPN	<b>dog</b>	HPHFVRCIIPN
<b>MYH10</b>	NPNFVRCIIPN		
<b>MYH11</b>	TPNFVRCIIPN		
<b>MYH13</b>	HPHFVRCIIPN		

FIG. 4. Conservation of Arg674 in *MYH8* paralogs and orthologs.

These results suggest that the etiologies of Carney complex and TPS are independent, and that the observation of both disorders segregating in a single pedigree is likely to be coincidental. *MYH8* appears to be expressed in the developing chick heart [Machida et al., 2000]. Therefore, it is possible that mutations in *MYH8* influence susceptibility to isolated cardiac myxoma. However, while our study was not designed to test the relationship between *MYH8* mutations and risk for cardiac myxoma, none of the individuals with TPS that we studied were

reported to have a cardiac myxoma. *MYH8* is expressed only in the perinatal period and primarily in the skeletal muscles of the limbs and to a more limited extent in the muscles of the face. Therefore, both the temporal and spatial expression of *MYH8* are consistent with the following: the contractures in TPS appear prenatally, are limited to the limbs and face, and are non-progressive. The spatial expression pattern of *MYH8* is similar to that of *MYH3*, the gene that encodes the fetal myosin heavy chain. Mutations in *MYH3* cause congenital contractures of

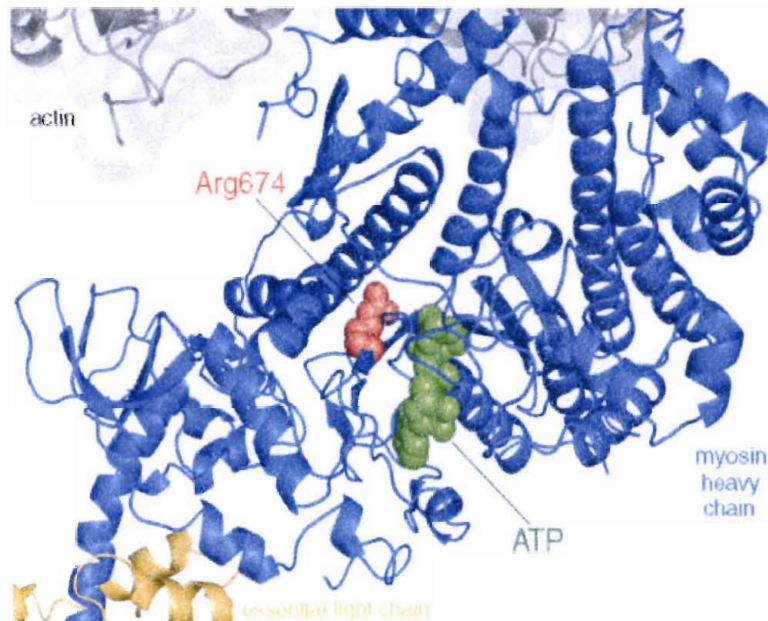


FIG. 5. Structural model of actin-myosin complex. The ribbon diagram of a short stretch of F-actin (gray) and myosin head (blue) is shown. The c.2021G > A mutation causes a substitution of the Arg674 (red) which is near the ATP binding site (an ATP molecule is shown in green).

the face and limbs in Freeman-Sheldon syndrome and Sheldon-Hall syndrome [Toydemir et al., 2006]. This observation confirms that these three distal arthrogryposis syndromes have shared pathogenesis and is consistent with the hypothesis that distal arthrogryposis syndromes are, in general, caused by disruption of the contractile complex of fast-twitch myofibers.

#### ACKNOWLEDGMENTS

We thank the individuals and their families for their participation and Frank Whitby for structure analysis. We are grateful to our study coordinator Ann Rutherford. This work was supported by the U.S. National Institutes of Health R01-HD048895, the U.S. Center for Disease Control, University of Utah Clinical Genetics Research Program, University of Utah Graduate Research Fellowship, and in part by the National Institute of Child Health and Human Development Intramural Program.

#### REFERENCES

- Adams C, Rees M. 1999. Congenital trismus secondary to masseteric fibrous bands: Endoscopically assisted exploration. *J Craniofac Surg* 10:375–379.
- Bamshad M, Jorde LB, Carey JC. 1996. A revised and extended classification of the distal arthrogryposes. *Am J Med Genet* 65:277–281.
- Carlos R, Contreras E, Cabrera J. 2005. Trismus-pseudocamptodactyly syndrome (Hecht-Beals' syndrome): Case report and literature review. *Oral Dis* 11:186–189.
- Chen H, Fowler M, Hogan GR, Lew D, Herbst J, Albright J. 1992. Trismus-Pseudocamptodactyly syndrome: Report of a family and review of literature with special consideration of morphological features. *Dysmorphology and Clinical Genetics* 6:165–174.
- De Jong JG. 1971. A family showing strongly reduced ability to open the mouth and limitation of some movements of the extremities. *Humangenetik* 13:210–217.
- DeLano WL. 2002. The PyMOL Molecular Graphics System.
- Geva D, Ezri T, Szmuk P, Gelman-Kohan Z, Shklar BZ. 1997. Anaesthesia for Hecht Beals syndrome. *Paediatr Anaesth* 7:178–179.
- Guimaraes AS, Marie SK. 2005. Dominant form of arthrogryposis multiplex congenita with limited mouth opening: A clinical and imaging study. *J Orofac Pain* 19:82–88.
- Hall JG, Reed SC, Greene G. 1982. The distal arthrogryposes: Delineation of new entities—review and nosologic discussion. *Am J Med Genet* 11:185–239.
- Hecht F, Beals RK. 1969. Inability to open the mouth fully: An autosomal dominant phenotype with facultative camptodactyly and short stature. In: Bergsma D, editor. *Birth defects: Original article series. Part III: Limb malformations, Vol. V*. New York: Alan R Liss for The National Foundation-March of Dimes, p 96–98.
- Hertrich K, Schuch H. 1991. Restricted mouth opening as a leading symptom of trismus-pseudocamptodactyly syndrome. *Dtsch Zahnärztl Z* 46:416–419.
- Hirano A, Iio Y, Murakami R, Fujii T. 1994. Recurrent trismus: Twenty-year follow-up result. *Cleft Palate Craniofac J* 31:309–312.
- Horowitz SL, McNulty EC, Chabora AJ. 1973. Limited intermaxillary opening—an inherited trait. *Oral Surg Oral Med Oral Pathol* 36:490–492.
- Karras SC, Wolford LM. 1995. Trismus-pseudocamptodactyly syndrome: Report of a case. *J Oral Maxillofac Surg* 53:80–84.
- Kirschner LS, Carney JA, Pack SD, Taymans SE, Giatzakis C, Cho YS, Cho-Chung YS, Stratakis CA. 2000. Mutations of the gene encoding the protein kinase A type I-alpha regulatory subunit in patients with the Carney complex. *Nat Genet* 26:89–92.
- Lano CFJ, Werkhaven J. 1997. Airway management in a patient with Hecht's syndrome. *South Med J* 90:1241–1243.
- Lefaiivre JF, Aitchison MJ. 2003. Surgical correction of trismus in a child with Hecht syndrome. *Ann Plast Surg* 50:310–314.
- Mabry CC, Barnett IS, Hutcheson MW, Sorenson HW. 1974. Trismus pseudocamptodactyly syndrome: Dutch-Kentucky syndrome. *J Pediatr* 85:503–508.
- Machida S, Matsuoka R, Noda S, Hiratsuka E, Takagaki Y, Oana S, Furutani Y, Nakajima H, Takao A, Momma K. 2000. Evidence for the expression of neonatal skeletal myosin heavy chain in primary myocardium and cardiac conduction tissue in developing chick heart. *Dev Dyn* 217:37–49.
- Markus AF. 1986. Limited mouth opening and shortened flexor muscle-tendon units: 'trismus-pseudocamptodactyly'. *Br J Oral Maxillofac Surg* 24:137–142.
- Mercuri LG. 1981. The Hecht, Beals, and Wilson syndrome: Report of case. *J Oral Surg* 39:53–56.
- Nagata O, Tateoka A, Shiuro R, Kimizuka M, Hanaoka K. 1999. Anaesthetic management of two paediatric patients with Hecht-Beals syndrome. *Paediatr Anaesth* 9:444–447.
- O'Brien PJ, Gropper PT, Tredwell SJ, Hall JG. 1984. Orthopaedic aspects of the trismus pseudocamptodactyly syndrome. *J Pediatr Orthop* 4:469–471.
- Pelo S, Boghi F, Moro A, Boniello R, Mosca R. 2003. Trismus-pseudocamptodactyly syndrome: A case report. *Eur J Paediatr Dent* 4:33–36.
- Rayment I, Holden HM, Whittaker M, Yohn CB, Lorenz M, Holmes KC, Milligan RA. 1993a. Structure of the actin-myosin complex and its implications for muscle contraction. *Science* 261:58–65.
- Rayment I, Rypniewski WR, Schmidt-Base K, Smith R, Tomchick DR, Benning MM, Winkelmann DA, Wesenberg G, Holden HM. 1993b. Three-dimensional structure of myosin subfragment-1: A molecular motor. *Science* 261:50–58.
- Robertson RD, Spence MA, Sparkes RS, Neiswanger K, Field LL. 1982. Linkage analysis with the trismus-pseudocamptodactyly syndrome. *Am J Med Genet* 12:115–120.
- Rombouts JJ, Verellen-Dumoulin C. 1992. Trismus-pseudocamptodactyly syndrome: Presentation and genealogy of a new European case. *Ann Chir Main Memb Super* 11:333–337.
- Seavello J, Hammer GB. 1999. Tracheal intubation in a child with trismus pseudocamptodactyly (Hecht) syndrome. *J Clin Anesth* 11:251–256.
- Skinner AM, Rees MJ. 2004. Congenital trismus secondary to masseteric fibrous bands: A 7-year follow-up report as an approach to management. *J Craniofac Surg* 15:709–713.
- Stratakis CA, Bertherat J, Carney JA. 2004. Mutation of perinatal myosin heavy chain. *N Engl J Med* 351:2556–2558.
- Teng RJ, Ho MM, Wang PJ, Hwang KC. 1994. Trismus-pseudocamptodactyly syndrome: Report of one case. *Zhonghua Min Guo Xiao Er Ke Yi Xue Hui Za Zhi* 35:144–147.
- Ter Haar BGA, Van Hoof RF. 1974. The Trismus-Pseudocamptodactyly syndrome. *J Med Genet* 11:41–49.
- Toydemir RM, Rutherford A, Whitby FG, Jorde LB, Carey JC, Bamshad MJ. 2006. Mutations in embryonic myosin heavy chain (*MYH3*) cause Freeman-Sheldon Syndrome. *Nat Genet* 38:561–565.
- Tsukahara M, Shinozaki F, Kajii T. 1985. Trismus-pseudocamptodactyly syndrome in a Japanese family. *Clin Genet* 28:247–250.
- Vaghadia H, Blackstock D. 1988. Anaesthetic implications of the trismus pseudocamptodactyly (Dutch-Kentucky or Hecht Beals) syndrome. *Can J Anaesth* 35:80–85.

- Veugelers M, Bressan M, McDermott DA, Weremowicz S, Morton CC, Mabry CC, Lefavre JF, Zunamon A, Destree A, Chaudron JM, Basson CT. 2004. Mutation of perinatal myosin heavy chain associated with a Carney complex variant. *N Engl J Med* 351:460-469.
- Wilson RV, Gaines DL, Brooks A, Carter TS, Nance WE. 1969. Autosomal dominant inheritance of shortening of the flexor profundus muscle-tendon unit with limitation of jaw excursion. In: Bergsma D, editor. *Birth defects: Original article series. Part III: Limb malformations, Vol. V.* New York: Alan R Liss for The National Foundation-March of Dimes. p 99-102.
- Yamashita DD, Arnet GF. 1980. Trismus-pseudocamptodactyly syndrome. *J Oral Surg* 38:625-630.

## CHAPTER 4

### A LOSS-OF-FUNCTION MUTATION IN *FGFR3* CAUSES CAMPTODACTYLY, TALL STATURE, AND HEARING LOSS (CATSHL) SYNDROME

The following chapter is a manuscript coauthored by myself, Anna E. Brassington, Pınar Bayrak-Toydemir, Patrycja A. Krakowiak, Lynn B. Jorde, Frank G. Whitby, Nicola Longo, and Michael J. Bamshad. This article is published in *American Journal of Human Genetics* in 2006 (volume 79, number 5, pages 935-941). It is presented here with the permission of the coauthors and the publisher.

## A Novel Mutation in *FGFR3* Causes Camptodactyly, Tall Stature, and Hearing Loss (CATSHL) Syndrome

Reha M. Toydemir, Anna E. Brassington, Pinar Bayrak-Toydemir, Patrycja A. Krakowiak, Lynn B. Jorde, Frank G. Whitby, Nicola Longo, David H. Viskochil, John C. Carey, and Michael J. Bamshad

Activating mutations of *FGFR3*, a negative regulator of bone growth, are well known to cause a variety of short-limbed bone dysplasias and craniosynostosis syndromes. We mapped the locus causing a novel disorder characterized by camptodactyly, tall stature, scoliosis, and hearing loss (CATSHL syndrome) to chromosome 4p. Because this syndrome recapitulated the phenotype of the *Fgfr3* knockout mouse, we screened *FGFR3* and subsequently identified a heterozygous missense mutation that is predicted to cause a p.R621H substitution in the tyrosine kinase domain and partial loss of *FGFR3* function. These findings indicate that abnormal *FGFR3* signaling can cause human anomalies by promoting as well as inhibiting endochondral bone growth.

Fibroblast growth factor receptor 3 (*FGFR3*) is one of five distinct membrane-spanning tyrosine kinases that participate in a variety of developmental processes. Mutations in *FGFR3* cause at least half a dozen different disorders, including achondroplasia (ACH [MIM 100800]), hypochondroplasia (HCH [MIM 146000]), thanatophoric dysplasia I and II (MIM 187600), Muenke syndrome (MIM 602849), Crouzon syndrome with acanthosis nigricans (MIM 187600), severe ACH with developmental delay and acanthosis nigricans (SADDAN) syndrome,<sup>1</sup> and lacrimo-auriculo-dental-digital (LADD [MIM 149730]) syndrome.<sup>2,3</sup> *FGFR3* is a negative regulator of bone growth, and all mutations characterized to date cause constitutive *FGFR3* activation and impair endochondral bone growth.<sup>3</sup>

We evaluated a large Utah pedigree in which 27 living affected family members spanning four generations (from a total of 35 affected individuals in seven generations; see fig. 1) were affected with dominantly inherited camptodactyly, tall stature, and hearing loss or CATSHL (pronounced "cat-shul") syndrome (fig. 2). Phenotypic information and DNA were available from 20 of 27 affected individuals. Adult height in males was >97th percentile in 5 of 5 men, with a mean height of 77 inches, and adult height in females was >75th percentile in 9 of 9 and >97th percentile in 8 of 9 women, with a mean height of 70 inches. Camptodactyly of the hands and/or feet (fig. 2) was present in 18 (90%) of 20 individuals, and 17 (85%) of 20 had hearing loss (14 of 20 were documented as having hearing loss, and 3 of 20 acknowledged having hearing loss but refused formal testing). Of 20 individuals, 12 (60%) had developmental delay and/or mental retardation, and several of these had microcephaly (head circumference <2nd percentile). Several had scoliosis and/or a

pectus excavatum (fig. 2), although the frequency of occurrence might be underestimated because many family members elected not to undergo chest and/or spine examination. No individual had characteristics of LADD syndrome or craniosynostosis syndromes caused by mutations in *FGFR3*. Marfan syndrome was considered a possible diagnosis, but no affected individuals who were examined had severe myopia, lens dislocation, or aortic-root abnormalities. Therefore, the diagnosis of Marfan syndrome was excluded.

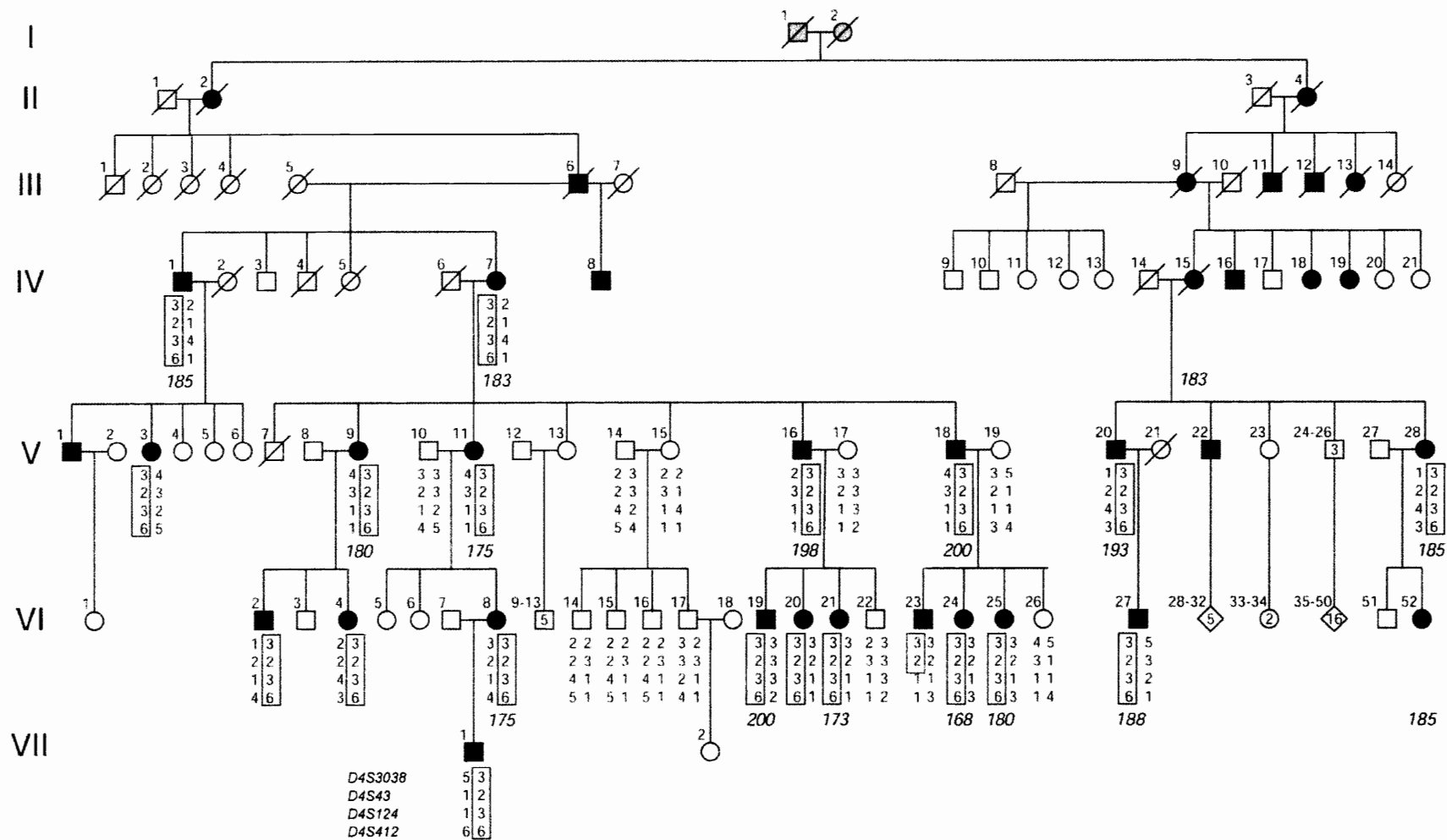
Radiographic findings included tall vertebral bodies with irregular borders and broad femoral metaphyses with long tubular shafts (data not shown). Several affected individuals had a single osteochondroma of the femur, the tibia, or a phalanx; pectus abnormalities; and/or severe thoracolumbar kyphoscoliosis (fig. 2). On audiological exam, each tested individual had bilateral sensorineural hearing loss and absent otoacoustic emissions (fig. 3). By report, the hearing loss was congenital or developed in early infancy, progressed variably in early childhood, and ranged from mild to severe. Computed tomography and magnetic resonance imaging revealed that the brain, middle ear, and inner ear were structurally normal.

To identify the locus for CATSHL syndrome, we performed a genomewide linkage scan, on 20 affected individuals, that revealed a significantly positive LOD score of 3.76 (recombination fraction  $|\theta|$  0.001) with marker *D4S412* (table 1), located on the tip of chromosome 4p. A multipoint LOD score estimated from markers saturating this region was 5.1 and reached its maximum at *D4S43* (table 2). No other region of the genome harbored markers with a significantly positive LOD score. Haplotype analysis delimited a critical interval of ~7 Mb (fig. 1) that contained

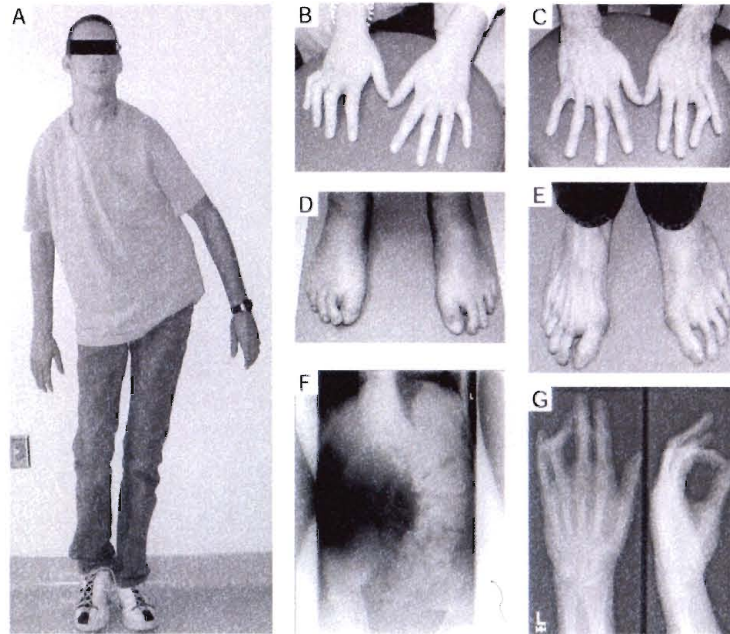
From the Departments of Human Genetics (R.M.T.; A.E.B.; L.B.J.), Pathology (P.B.T.), Biochemistry (F.G.W.), and Pediatrics (N.L.; D.H.V.; J.C.C.), University of Utah, Salt Lake City; Department of Pediatrics, University of Arkansas for Medical Sciences, Little Rock (P.A.K.); and Departments of Pediatrics and Genome Sciences, University of Washington (M.J.B.), and Children's Hospital and Regional Medical Center (M.J.B.), Seattle

Received June 14, 2006; accepted for publication August 10, 2006; electronically published September 26, 2006.

Address for correspondence and reprints: Dr. Michael J. Bamshad, Department of Pediatrics, Division of Genetics and Developmental Medicine, University of Washington School of Medicine, 1959 NE Pacific Street, HSB RR349, Seattle, WA 98195. E-mail: mbamshad@u.washington.edu  
*Am. J. Hum. Genet.* 2006;79:935–941. © 2006 by The American Society of Human Genetics. All rights reserved. 0002-9297/2006/7905-0015\$15.00



**Figure 1.** Pedigree of the family with CATSHL syndrome. Filled symbols indicate either affected individuals (*black*) or individuals of unknown status (*gray*), and open symbols indicate unaffected individuals. Genotypes for *D4S3038*, *D4S43*, *D4S124*, and *D4S412* are listed, and the disease haplotype segregating with each affected individual is boxed. The height (in centimeters) of each affected adult is indicated in italics.



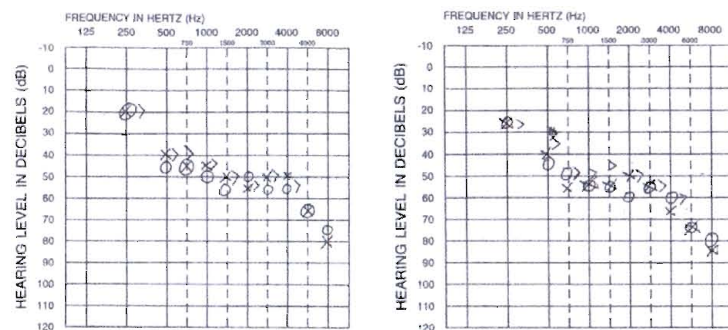
**Figure 2.** Clinical characteristics of CATSHL syndrome. *A*, Tall stature, pectus excavatum, and scoliotic deformity of the spine. Camptodactyly of the hands (*B* and *C*) and feet (*D* and *E*). *F*, Anterior-posterior radiograph of the thoracolumbar spine, showing  $\sim 80^\circ$  lateral curvature of the lumbar spine. *G*, Radiograph of the hand of an individual with camptodactyly.

$\sim 30$  genes, including *FGFR3* (Genbank accession number NM\_000142). Because the features of CATSHL syndrome overlapped with those of mice homozygous for a *Fgfr3* null allele,<sup>4,5</sup> we screened affected individuals for *FGFR3* mutations by direct DNA sequencing.

In all affected family members tested ( $n = 20$ ), we discovered a G $\rightarrow$ A missense mutation at nucleotide position +1862 (c.1862G $\rightarrow$ A) that creates a novel *Dra*III restriction site (fig. 4) and a histidine $\rightarrow$ arginine substitution (p.R621H). R621 is located in the catalytic loop of the

tyrosine kinase domain of FGFR3, and it is invariant in the tyrosine kinase superfamily (fig. 4c). No unaffected family members had this variant, nor was it found in 500 chromosomes from individuals matched for geographic ancestry (Western Europe).

The catalytic loop plays a critical role in the transfer of a phosphate ion to its target sites. On the basis of homology modeling done using the crystal structure of FGFR1, the homologous amino acid residue (i.e., R627) is predicted to be critical for the transfer of phosphate.<sup>6</sup> The



**Figure 3.** Representative audiograms of two individuals with CATSHL syndrome that demonstrate sensorineural hearing loss. Pure-tone response in the left ear is indicated by a cross ( $\times$ ) and response in the right ear by an open circle ( $\circ$ ). Responses in the 500–8,000 Hz range were obtained in the mild sloping to severe hearing loss range, bilaterally.



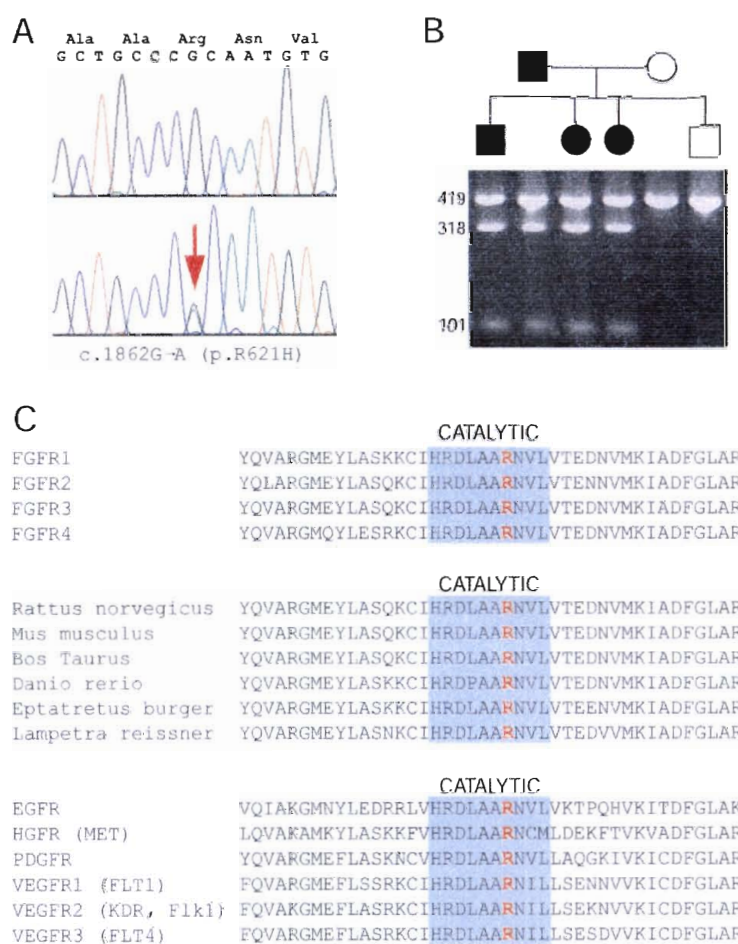
p.R621H substitution may therefore interfere with the ability of FGFR3 to transfer phosphate to its peptide substrate, resulting in loss of function (fig. 5). This prediction is supported by experiments in which site-directed mutagenesis of the homologous amino acid residue in the kinase domain of the insulin receptor (i.e., R1136) and the C-terminal Src Kinase virtually inactivates the receptor.<sup>7,8</sup>

The anomalies observed in humans with p.R621H recapitulate the defects identified in *Fgfr3*<sup>-/-</sup> mice.<sup>4,5</sup> The skeletal phenotype of *Fgfr3*<sup>-/-</sup> mice is characterized by elongated long bones (particularly the femur) and long vertebral bodies that predispose the animals to thoracic kyphoscoliosis and tail kinks. Like the *Fgfr3*<sup>-/-</sup> mice, only

**Table 1. Two-Point Linkage Data for All Chromosomes**

The table is available in its entirety in the online edition of *The American Journal of Human Genetics*.

bones formed by endochondral ossification are affected in CATSHL syndrome, and the bones most notably affected are the long bones and vertebral bodies. *Fgfr3*<sup>-/-</sup> mice also exhibit profound sensorineural deafness that is caused by cochlear defects, including absence of inner and outer pillar cells in the organ of Corti and reduced innervation of the outer hair cells.<sup>4,5</sup> However, the middle



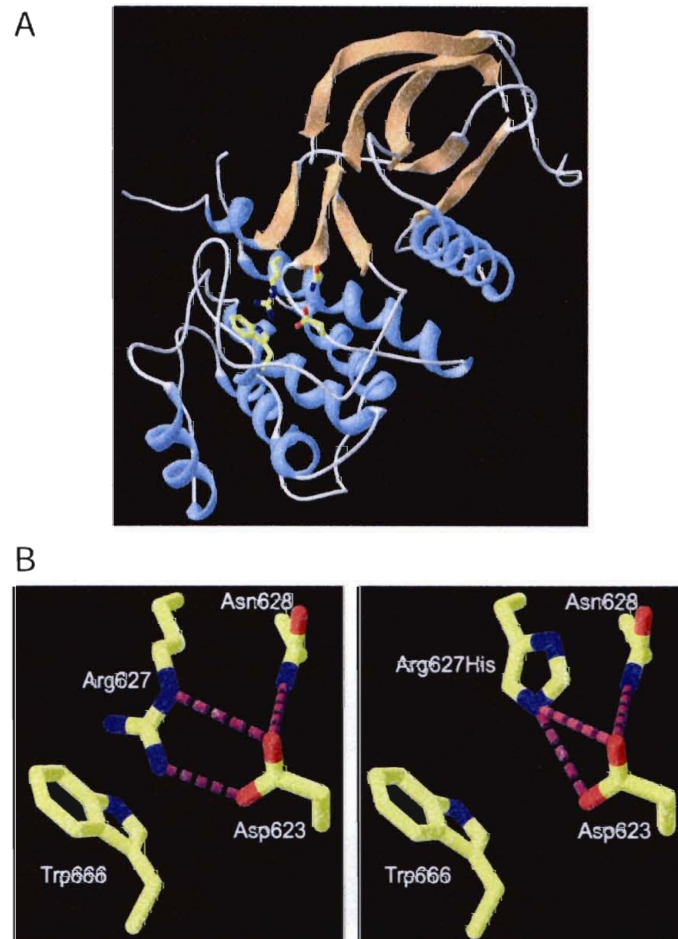
**Figure 4.** Identification of loss-of-function mutation in *FGFR3* that causes CATSHL syndrome. **A**, A heterozygous G→A *FGFR3* mutation creates a novel *Dra*III restriction site. **B**, Restriction digest with *Dra*III that confirmed homozygosity for the uncut wild-type *FGFR3* allele (419 bp) in unaffected individuals (open symbols), whereas affected individuals (filled symbols) were heterozygous for a wild-type allele (419 bp) and a mutant allele that cut into two fragments (318 and 101 bp). **C**, Amino acid alignment of different FGFRs. Arginine at codon 621 of the activation domain is conserved among human FGFR1, -2, -3, and -4 (top), in all vertebrate FGFR3s characterized to date (middle), and in other receptor tyrosine kinases (bottom).

ear ossicles and the gross structure of the inner ear of *Fgfr3*<sup>-/-</sup> mice are normal. Likewise, individuals with p.R621H had sensorineural hearing loss, normal conductive hearing, and no gross abnormalities of the middle or inner ear. In contrast to the static deafness observed in *Fgfr3*<sup>-/-</sup> mice, the hearing loss in individuals with the p.R621H substitution was progressive. This difference may be a result of the residual activity of the wild-type copy of *FGFR3* in individuals with CATSHL syndrome. It also suggests that the support cells of the organ of Corti might require *FGFR3* for maintenance as well as formation, an inference consistent with the expression of *Fgfr3* in pillar cells of the adult rat.<sup>9</sup> This requirement may be dose-sensitive, because some individuals with constitutively activating mutations in *FGFR3* also develop sensorineural hearing loss.<sup>10</sup>

**Table 2. Results of the Multipoint Linkage Analysis**

The table is available in its entirety in the online edition of *The American Journal of Human Genetics*.

The skeletal phenotypes of both *Fgfr3*<sup>-/-</sup> mice and individuals with CATSHL syndrome also are similar to those of sheep with a naturally occurring condition called "ovine hereditary chondrodysplasia" or "spider lamb syndrome" (SLS).<sup>11,12</sup> SLS is a codominant condition characterized by modestly increased long-bone length in heterozygotes and elongated "spider-like" legs, a "humped and twisted spine," flexion contractures of the legs, and deformed ribs and sternebra in homozygotes.<sup>12</sup> SLS is caused by a substitution of glutamic acid for valine at



**Figure 5.** A, Ball-and-stick model of the active-site region of the catalytic domain of FGFR1. The model is based on the 0.2-nm crystal structure of the tyrosine kinase domain of the human FGFR1 (RSCB Protein Data Bank entry 1FGK). R627 of FGFR1 is homologous to R621 of FGFR3. B, Hypothetical model of FGFR3, showing position of histidine side chain when substituted for R621.

amino acid position 700 (p.V700E) in the tyrosine kinase of *Fgfr3*, where it is predicted to cause a loss of *FGFR3* function.<sup>12</sup> Therefore, both p.R621H and p.V700E cause a dominantly inherited loss of *FGFR3* function and similar skeletal anomalies.

For several reasons, it is unlikely that the loss of function caused by p.R621H results from haploinsufficiency. First, mice heterozygous for an *Fgfr3* null allele are phenotypically normal.<sup>4,5</sup> Second, deletion of *FGFR3*, which occurs in most patients with Wolf-Hirschhorn syndrome (WHS [MIM 194190]), is not associated with any of the skeletal defects observed in the individuals with p.R621H.<sup>13</sup> However, it is possible that other genes that are typically deleted in patients with WHS mask the effect of *FGFR3* hemizygosity. Third, the fibroblasts of individuals affected with CATSHL syndrome express both wild-type and mutant (i.e., p.R621H-containing) *FGFR3* RNA in nearly equal proportions, and the expression levels of all five FGFRs in patients are similar to those of normal individuals. Furthermore, both mutant and wild-type *FGFR3* localizes to its normal position in the cell membrane (data not shown). These observations suggest that p.R621H might, instead, cause loss of *FGFR3* function by a dominant negative mechanism.

Proper FGF signaling requires dimerization of *FGFR* molecules on the cell surface. Dimerization subsequently promotes the intracellular autophosphorylation of critical tyrosine residues in the activation loop of the receptor.<sup>6</sup> This stabilizes the tyrosine kinase domain in the active conformation, leading to phosphorylation of other tyrosine residues in the activation domain and binding of target proteins. p.R621H-*FGFR3* might form a heterodimer with wild-type *FGFR3* that reduces or abolishes kinase activity. This mechanism has been shown to underlie the dominant negative effect of several amino acid substitutions in the activation domain of the insulin receptor (MIM 147670), another tyrosine kinase receptor, that cause dominantly inherited insulin resistance.<sup>14,15</sup>

It has been speculated that polymorphisms in *FGFR3* might influence adult height.<sup>16</sup> This hypothesis is supported by the observation that several *FGFR3* mutations cause such mild forms of HCH that the height of affected individuals falls within the normal spectrum.<sup>16</sup> On the other hand, p.V700E is positively correlated with long-bone length in sheep, and the height of p.R621H heterozygotes overlaps with individuals on the taller end of the normal height spectrum. Analogous to the positive association between the level of *FGFR3* activation and bone-growth inhibition (i.e., higher levels of *FGFR3* activation cause more-severe limb shortening), our results indicate that increases in long-bone length are associated with *FGFR3* impairment. This observation suggests that human stature might be influenced by *FGFR3* activity in a dose-dependent fashion.

## Acknowledgments

We thank the individuals and family with this condition for their participation. We thank H. Coon, M. Page, A. Rutherford, R. Sanders, and R. Wiggins, for resources and technical assistance and G. Bellus, S. Mansour, A. Moon, and T. Wright, for comments and suggestions on the manuscript. This work was supported by National Institutes of Health grants HD-048895 and RR-00064, Centers for Disease Control grant U50/CCU822097-02, the Clinical Genetic Research Program at the University of Utah, the Primary Children's Medical Center Foundation, and the Children's Hospital and Regional Medical Center. R.M.T. is a recipient of the University of Utah Graduate Research Fellowship.

## Web Resources

Accession numbers and URLs for data presented herein are as follows:

GenBank, <http://www.ncbi.nlm.nih.gov/Genbank/> (for *FGFR3* cDNA [accession number NM\_000142])  
 Online Mendelian Inheritance in Man (OMIM), <http://www.ncbi.nlm.nih.gov/Omim/> (for ACH, HCH, thanatophoric dysplasia I and II, Muenke syndrome, Crouzon syndrome with acanthosis nigricans, LADD syndrome, WHS, and insulin receptor)  
 RSCB Protein Data Bank, <http://www.rcsb.org/pdb/Welcomedo> (for human *FGFR1* [entry 1FGK])

## References

1. Wilkie AOM, Patey SJ, Kan SH, van den Ouweland AMW, Hamel BCJ (2002) FGFs, their receptors, and human limb malformations: clinical and molecular correlations. *Am J Med Genet* 112:266–278
2. Rohmann E, Brunner HG, Kayserili H, Uyguner O, Nurnberg G, Lew ED, Dobbie A, Eswarakumar VP, Üzümcü A, Ulubil-Emeroglu M, Leroy JG, Li Y, Becker C, Lehnerdt K, Cremers CW, Yüksel-Apak M, Nurnberg P, Kubisch C, Schlessinger J, van Bokhoven H, Wollnik B (2006) Mutations in different components of FGF signaling in LADD syndrome. *Nat Genet* 38:414–417
3. Tavormina PI, Bellus GA, Webster MK, Bamshad MJ, Fraley AE, McIntosh I, Szabo J, Jiang W, Jabs EW, Wilcox WR, Was-muth JJ, Donoghue DJ, Thompson LM, Francomano CA (1999) A novel skeletal dysplasia with developmental delay and acanthosis nigricans is caused by a Lys650Met mutation in the fibroblast growth factor receptor 3 gene. *Am J Hum Genet* 64:722–731
4. Deng C, Wynshaw-Boris A, Zhou F, Kuo A, Leder P (1996) Fibroblast growth factor receptor 3 is a negative regulator of bone growth. *Cell* 84:911–921
5. Colvin JS, Bohne BA, Harding GW, McEwen DG, Ornitz DM (1996) Skeletal overgrowth and deafness in mice lacking fibroblast growth factor receptor 3. *Nat Genet* 12:390–397
6. Mohammadi M, Schlessinger J, Hubbard SR (1996) Structure of the FGF receptor tyrosine kinase domain reveals a novel autoinhibitory mechanism. *Cell* 86:577–587
7. Ablooglu AJ, Frankel M, Rusinova E, Alexander Ross JB, Kohanski RA (2001) Multiple activation loop conformations and their regulatory properties in the insulin receptor's kinase domain. *J Biol Chem* 276:46933–46940
8. Williams DM, Wang D, Cole PA (2000) Chemical rescue of a

- mutant protein-tyrosine kinase. *J Biol Chem* 275:38127–38130
9. Pirvola U, Cao Y, Oellig C, Suoqiang Z, Pettersson RF, Ylikoski J (1995) The site of action of neuronal acidic fibroblast growth factor is the organ of Corti of the rat cochlea. *Proc Natl Acad Sci USA* 92:9269–9273
  10. Muenke M, Gripp KW, McDonald-McGinn DM, Gaudenz K, Whitaker LA, Bartlett SP, Markowitz RI, et al. (1997) A unique point mutation in the fibroblast growth factor receptor 3 gene (*FGFR3*) defines a new craniosynostosis syndrome. *Am J Hum Genet* 60:555–564
  11. Beever JE, Smit MA, Meyers SN, Hadfield TS, Bottema C, Albretsen J, Cockett NE (2006) A single-base change in the tyrosine kinase II domain of ovine *FGFR3* causes hereditary chondrodysplasia in sheep. *Anim Genet* 37:66–71
  12. Vanek JA, Walter PA, Alstad AD (1989) Radiographic diagnosis of hereditary chondrodysplasia in newborn lambs. *J Am Vet Med Assoc* 194:244–248
  13. Wright TJ, Ricke DO, Denison K, Abmayr S, Cotter PD, Hirschhorn K, Keinanen M, McDonald-McGinn D, Somer M, Spinner N, Yang-Feng T, Zackai E, Altherr MR (1997) A transcript map of the newly defined 165 kb Wolf-Hirschhorn syndrome critical region. *Hum Mol Genet* 6:317–324
  14. Chang PY, Benecke H, Le Marchand-Brustel Y, Lawitts J, Moller DE (1994) Expression of a dominant-negative mutant human insulin receptor in the muscle of transgenic mice. *J Biol Chem* 269:16034–16040
  15. Rau H, Kocova M, O’Rahilly S, Whitehead JP (2000) Naturally occurring amino acid substitutions at Arg1174 in the human insulin receptor result in differential effects on receptor biosynthesis and hybrid formation, leading to discordant clinical phenotypes. *Diabetes* 49:1264–1268
  16. Bellus GA, Spector EB, Speiser PW, Weaver CA, Garber AT, Bryke CR, Israel J, Rosengren SS, Webster MK, Donoghue DJ, Francomano CA (2000) Distinct missense mutations of the *FGFR3* Lys650 codon modulate receptor kinase activation and the severity of the skeletal dysplasia phenotype. *Am J Hum Genet* 67:1411–1421

Table 4.1. Two-Point Linkage Data for All Chromosomes

Chromosome and Marker	LOD at $=\theta$						
	0.00	0.01	0.05	0.10	0.20	0.30	0.40
1:							
<i>DIS407</i>	-8.31	-3.36	-1.70	-0.98	-0.36	-0.11	-0.02
<i>DIS396</i>	-18.90	-4.72	-2.44	-1.45	-0.54	-0.14	0.01
<i>DIS1150</i>	-9.94	-6.38	-3.76	-2.47	-1.21	-0.55	-0.17
<i>DIS1162</i>	-7.09	-3.57	-2.11	-1.44	-0.74	-0.35	-0.11
<i>DIS410</i>	-5.60	-3.00	-1.99	-1.47	-0.94	-0.59	-0.29
<i>DIS406</i>	-7.05	-5.43	-3.26	-2.24	-1.23	-0.67	-0.29
<i>DIS1174</i>	-7.19	-5.10	-2.90	-1.91	-1.04	-0.59	-0.26
<i>DIS1153</i>	-11.15	-6.18	-4.84	-3.39	-1.77	-0.92	-0.38
<i>DIS1165</i>	-16.48	-6.43	-3.53	-2.27	-1.08	-0.48	-0.15
<i>DIS370</i>	-13.00	-1.93	-0.64	-0.18	0.13	0.19	0.13
<i>DIS384</i>	-10.80	-0.70	0.13	0.48	0.67	0.60	0.37
<i>DIS408</i>	-5.54	-2.18	-1.31	-0.88	-0.46	-0.24	-0.10
<i>DIS373</i>	-14.13	-2.71	-1.15	-0.48	0.07	0.23	0.19
<i>DIS1164</i>	-5.71	-2.34	-1.44	-1.00	-0.53	-0.27	-0.10
<i>DIS399</i>	-0.12	-0.12	-0.10	-0.08	-0.04	-0.02	0.00
<i>DIS389</i>	-10.87	-1.65	-0.27	0.20	0.44	0.39	0.24
<i>DIS517</i>	-21.05	-6.02	-3.05	-1.77	-0.67	-0.21	-0.03
<i>DIS404</i>	-7.73	-3.39	-1.75	-0.99	-0.32	-0.05	0.04
<i>DIS211</i>	-18.09	-8.51	-5.11	-3.44	-1.77	-0.88	-0.33
2:							
<i>D2S262</i>	-16.13	-5.90	-3.18	-2.04	-1.03	-0.53	-0.22
<i>D2S272</i>	-15.04	-5.59	-2.89	-1.78	-0.78	-0.31	-0.08
<i>D2S265</i>	-5.63	-2.40	-1.10	-0.61	-0.24	-0.11	-0.06
<i>D2S1248</i>	-12.95	-5.42	-2.60	-1.45	-0.51	-0.15	-0.02
<i>D2S1262</i>	0.17	0.17	0.15	0.12	0.07	0.03	0.01
<i>D2S274</i>	-16.98	-4.69	-2.08	-1.12	-0.39	-0.14	-0.04
<i>D2S1265</i>	-11.21	-2.75	-1.26	-0.64	-0.15	0.02	0.05
<i>D2S275</i>	-20.46	-5.61	-2.75	-1.58	-0.58	-0.18	-0.04
<i>D2S1268</i>	-4.42	-1.08	-0.27	0.07	0.28	0.27	0.16
<i>D2S1244</i>	-13.82	-6.01	-3.09	-1.83	-0.73	-0.26	-0.06
<i>D2S273</i>	-10.56	-2.84	-1.47	-0.90	-0.39	-0.15	-0.03
<i>D2S1242</i>	-16.27	-5.38	-2.93	-1.88	-0.90	-0.42	-0.15
<i>D2S1279</i>	-18.57	-5.16	-2.86	-1.82	-0.81	-0.31	-0.07
3:							
<i>D3S1539</i>	-4.69	-0.64	-0.01	0.20	0.30	0.26	0.15
<i>D3S1537</i>	-4.33	-0.99	-0.19	0.14	0.35	0.34	0.22
<i>D3S2303</i>	-13.19	-3.81	-1.68	-0.82	-0.15	0.08	0.10
<i>D3S2327</i>	-7.22	-1.56	-0.17	0.32	0.56	0.46	0.24
<i>D3S2304</i>	-6.27	-4.51	-2.72	-1.83	-0.90	-0.41	-0.13
<i>D3S1514</i>	-14.59	-3.20	-1.25	-0.54	-0.03	0.11	0.09

Table 4.1. Continued

Chromosome and Marker	LOD at $=\theta$						
	0.00	0.01	0.05	0.10	0.20	0.30	0.40
<i>D3S2329</i>	-6.88	-1.13	-.48	-0.25	-0.09	-0.03	0.00
<i>D3S1542</i>	-16.77	-5.28	-2.86	-1.76	-0.74	-0.26	-0.05
<i>D3S2318</i>	-4.31	-1.03	-0.39	-0.18	-0.06	-0.02	0.00
<i>D3S1667</i>	-19.00	-7.21	-5.50	-3.87	-2.10	-1.12	-0.47
<i>D3S2322</i>	-13.33	-5.50	-4.77	-3.53	-1.92	-1.01	-0.41
<i>D3S1512</i>	-3.90	-3.85	-2.57	-1.75	-0.99	-0.58	-0.27
<i>D3S1545</i>	-6.52	-5.80	-4.15	-2.88	-1.60	-0.88	-0.38
<i>D3S1530</i>	-12.12	-6.55	-3.67	-2.38	-1.17	-0.56	-0.21
<i>D3S2305</i>	-14.58	-8.47	-5.23	-3.42	-1.73	-0.86	-0.34
4:							
<i>D4S3360</i>	1.07	1.04	0.92	0.77	0.48	0.25	0.09
<i>D4S3038</i>	3.72	3.65	3.36	2.99	2.21	1.43	0.68
<i>D4S412</i>	3.76	3.68	3.34	2.90	2.04	1.21	0.48
<i>D4S3023</i>	1.81	1.76	1.58	1.37	0.98	0.64	0.32
<i>D4S2285</i>	0.22	0.21	0.18	0.13	0.04	0.01	0.00
<i>D4S431</i>	2.12	2.07	1.87	1.62	1.16	0.74	0.36
<i>D4S3007</i>	-9.34	-1.65	-0.43	-0.04	0.15	0.14	0.08
<i>D4S1511</i>	-3.33	-0.62	0.12	0.37	0.45	0.33	0.16
<i>D4S1525</i>	-4.34	-0.72	0.07	0.37	0.51	0.42	0.24
<i>D4S2289</i>	-17.89	-6.69	-3.81	-2.51	-1.22	-0.57	-0.21
<i>D4S2282</i>	-19.67	-8.67	-4.75	-3.00	-1.42	-0.67	-0.25
<i>D4S2295</i>	-5.44	-5.35	-3.79	-2.62	-1.42	-0.74	-0.30
<i>D4S1631</i>	-13.56	-7.69	-5.13	-3.40	-1.72	-0.84	-0.32
<i>D4S2308</i>	-16.06	-8.84	-5.57	-3.65	-1.83	-0.90	-0.34
<i>D4S1517</i>	-8.37	-7.41	-4.86	-3.24	-1.71	-0.91	-0.38
<i>D4S2284</i>	-16.72	-3.97	-1.99	-1.22	-0.57	-0.26	-0.09
<i>D4S1531</i>	-5.47	-5.37	-3.72	-2.56	-1.38	-0.72	-0.30
<i>D4S1527</i>	0.18	0.17	0.15	0.12	0.07	0.03	0.01
<i>D4S2286</i>	-19.82	-4.23	-1.73	-0.78	-0.05	0.17	0.17
<i>D4S1515</i>	-19.69	-5.91	-2.67	-1.42	-0.41	-0.03	0.08
<i>D4S2292</i>	-16.65	-3.42	-1.50	-0.75	-0.13	0.10	0.12
<i>D4S1529</i>	-16.01	-5.20	-2.52	-1.47	-0.60	-0.23	-0.06
<i>D4S1530</i>	-14.94	-3.61	-1.56	-0.75	-0.09	0.12	0.13
<i>D4S2299</i>	-11.69	-3.60	-1.68	-0.97	-0.34	-0.06	0.03
5:							
<i>D5S593</i>	-16.18	-5.31	-2.67	-1.64	-0.80	-0.42	-0.19
<i>D5S580</i>	-13.41	-6.12	-5.40	-3.96	-2.16	-1.16	-0.05
<i>D5S1377</i>	-19.84	-7.28	-3.80	-2.35	-1.06	-0.47	-0.16
<i>D5S612</i>	-12.72	-6.45	-3.55	-2.29	-1.14	-0.56	-0.22
<i>D5S1351</i>	-12.96	-7.06	-5.56	-3.95	-2.08	-1.10	-0.47
<i>D5S1347</i>	-0.62	-0.51	-0.26	-0.13	-0.04	-0.02	-0.01

Table 4.1. Continued

Chromosome and Marker	LOD at $=\theta$						
	0.00	0.01	0.05	0.10	0.20	0.30	0.40
<i>D5S1346</i>	-12.59	-8.95	-5.43	-3.62	-1.92	-1.02	-0.43
<i>D5S592</i>	-12.15	-5.75	-2.92	-2.92	-1.73	-0.69	-0.24
<i>D5S613</i>	-18.40	-8.51	-4.65	-2.94	-1.36	-0.59	-0.18
<i>D5S1392</i>	-12.36	-6.07	-3.38	-2.17	-1.03	-0.46	-0.15
<i>D5S1349</i>	-11.17	-5.57	-2.78	-1.67	-0.76	-0.35	-0.12
<i>D5S1398</i>	-11.19	-3.83	-1.74	-0.94	-0.34	-0.12	-0.02
<i>D5S1354</i>	-5.69	-2.16	-0.94	-0.47	-0.11	0.01	0.03
<i>FBN2</i>	-1.60	-1.05	-0.51	-0.30	-0.14	-0.06	-0.02
6:							
<i>D6S942</i>	-17.17	-4.92	-2.51	-1.48	-0.56	-0.16	0.01
<i>D6S399</i>	-5.23	-1.08	-0.45	-0.23	-0.07	-0.02	0.00
<i>D6S394</i>	-6.78	-1.01	0.19	0.54	0.63	0.45	0.20
<i>D6S400</i>	-6.76	-0.63	0.02	0.26	0.40	0.37	0.22
<i>D6S948</i>	-8.78	-5.39	-2.76	-1.70	-0.79	-0.37	-0.14
<i>D6S395</i>	-12.19	-7.84	-4.65	-3.04	-1.52	-0.75	-0.30
<i>D6S954</i>	-17.04	-8.27	-4.36	-2.72	-1.26	-0.58	-0.22
<i>D6S939</i>	-10.07	-6.59	-3.32	-2.01	-0.91	-0.41	-0.15
<i>D6S979</i>	-4.81	-2.11	-1.11	-0.64	-0.24	-0.07	-0.01
<i>D6S935</i>	-14.81	-4.69	-2.17	-1.20	-0.43	-0.12	0.00
<i>D6S393</i>	-16.61	-6.76	-3.83	-2.52	-1.24	-0.56	-0.18
<i>D6S392</i>	-16.44	-3.81	-1.66	-0.79	-0.11	0.12	0.13
<i>D6S1011</i>	-4.63	-0.61	-0.01	0.16	0.21	0.13	0.04
<i>D6S439</i>	-15.87	-2.73	-1.22	-0.57	-0.01	0.19	0.18
<i>D6S291</i>	-10.86	-0.72	0.07	0.40	0.60	0.55	0.35
<i>D6S105</i>	-4.06	-0.72	0.07	0.37	0.51	0.42	0.24
<i>D6S276</i>	-0.08	-0.08	-0.06	-0.05	-0.03	-0.01	0.00
<i>509-8B2</i>	-11.50	-7.27	-4.38	-2.84	-1.42	-0.71	-0.29
<i>509-12B1</i>	-11.50	-7.27	-4.38	-2.84	-1.42	-0.71	-0.29
7:							
<i>D7S1484</i>	-12.19	-7.84	-4.65	-3.04	-1.52	-0.75	-0.30
<i>D7S620</i>	-17.17	-4.92	-2.51	-1.48	-0.56	-0.16	0.01
<i>D7S1504</i>	-6.76	-0.63	0.02	0.26	0.40	0.37	0.22
<i>D7S1512</i>	-11.50	-7.27	-4.38	-2.84	-1.42	-0.71	-0.29
<i>D7S1526</i>	-4.06	-0.72	0.07	0.37	0.51	0.42	0.24
<i>D7S1485</i>	-16.61	-6.76	-3.83	-2.52	-1.24	-0.56	-0.18
<i>D7S1517</i>	-11.72	-5.91	-3.49	-2.36	-1.26	-0.68	-0.29
<i>D7S1520</i>	-11.50	-7.27	-4.38	-2.84	-1.42	-0.71	-0.29
<i>D7S618</i>	-0.08	-0.08	-0.06	-0.05	-0.03	-0.01	0.00
<i>D7S1522</i>	-17.13	-7.57	-4.16	-2.67	-1.32	-0.64	-0.24
8:							
D8S391/D8S307	-12.02	-2.17	-0.82	-0.29	0.12	0.21	0.16

Table 4.1. Continued

Chromosome and Marker	LOD at $=\theta$						
	0.00	0.01	0.05	0.10	0.20	0.30	0.40
<i>D8S492</i>	-19.05	-4.64	-1.79	-0.67	0.17	0.39	0.30
<i>D8S405</i>	-0.16	0.35	0.76	0.80	0.64	0.41	0.20
<i>D8S499</i>	-13.98	-5.10	-2.36	-1.24	-0.29	0.07	0.14
<i>D8S1097</i>	-10.06	-2.82	-1.44	-0.88	-0.37	-0.13	-0.02
<i>D8S366</i>	-19.19	-3.21	-1.24	-0.51	0.04	0.19	0.17
<i>D8S562</i>	-8.68	-5.57	-3.03	-1.87	-0.88	-0.43	-0.18
<i>D8S343</i>	-12.98	-7.50	-4.17	-2.65	-1.24	-0.55	-0.17
<i>D8S384</i>	-6.49	-4.92	-2.74	-1.77	-0.85	-0.40	-0.14
<i>D8S378</i>	-23.90	-10.12	-5.31	-3.28	-1.46	-0.62	-0.19
<i>D8S386</i>	-15.01	-4.21	-2.04	-1.14	-0.37	-0.07	0.03
<i>D8S315</i>	-11.65	-4.35	-1.90	-0.90	-0.15	0.06	0.06
9:							
<i>D9S759</i>	-32.37	-12.01	-6.93	-4.53	-2.26	-1.09	-0.40
<i>D9S770</i>	-15.35	-6.85	-3.92	-2.61	-1.34	-0.66	-0.24
<i>D9S235</i>	-6.13	-1.44	-0.75	-0.46	-0.19	-0.07	-0.01
<i>D9S248</i>	-12.64	-5.99	-3.22	-2.06	-0.98	-0.44	-0.15
<i>D9S768</i>	-14.62	-3.84	-1.85	-1.08	-0.43	-0.17	-0.04
<i>D9S249</i>	-6.21	-3.91	-2.07	-1.28	-0.56	-0.22	-0.05
<i>D9S774</i>	-5.55	-3.62	-1.72	-1.04	-0.55	-0.35	-0.17
<i>D9S762</i>	-8.14	-4.26	-2.54	-1.61	-0.71	-0.28	-0.07
<i>D9S752</i>	-17.60	-4.33	-1.70	-0.71	0.03	0.23	0.19
<i>D9S15</i>	-8.35	-0.78	-0.17	0.02	0.10	0.07	0.02
10:							
<i>D10S526</i>	-8.21	-4.22	-2.13	-1.22	-0.42	-0.09	0.02
<i>D10S1152</i>	-26.40	-8.78	-4.60	-2.85	-1.28	-0.55	-0.17
<i>D10S527</i>	-5.18	-3.79	-2.25	-1.53	-0.83	-0.44	-0.19
<i>D10S509</i>	-25.19	-8.98	-4.77	-3.02	-1.41	-0.62	-0.18
<i>D10S524</i>	-3.48	-0.22	0.32	0.42	0.36	0.23	0.11
<i>D10S523</i>	-19.32	-5.38	-2.68	-1.61	-0.67	-0.25	-0.06
<i>D10S521</i>	-14.28	-8.63	-6.02	-4.04	-2.12	-1.09	-0.44
<i>D10S528</i>	-11.23	-4.84	-2.23	-1.26	-0.52	-0.24	-0.09
<i>D10S1134</i>	-12.69	-8.11	-6.11	-4.20	-2.23	-1.14	-0.45
11:							
<i>D11S1923</i>	-10.56	-6.38	-4.16	-2.84	-1.52	-0.79	-0.32
<i>D11S1301</i>	-15.36	-4.61	-1.97	-0.96	-0.16	0.09	0.12
<i>D11S1298</i>	-18.45	-7.48	-3.94	-2.43	-1.06	-0.42	-0.10
<i>D11S1291</i>	-16.77	-6.03	-2.77	-1.49	-0.45	-0.05	0.07
<i>D11S1302</i>	-12.23	-2.08	-0.73	-0.26	0.02	0.06	0.02
<i>D11S1899</i>	-9.74	-2.33	-1.11	-0.71	-0.39	-0.21	-0.07
<i>D11S1304</i>	-5.68	-4.70	-4.28	-3.91	-2.37	-1.37	-0.63



Table 4.1. Continued

Chromosome and Marker	LOD at $=\theta$						
	0.00	0.01	0.05	0.10	0.20	0.30	0.40
12:							
<i>VWFII</i>	-4.72	-2.71	-1.24	-0.66	-0.21	-0.07	-0.02
<i>D12S369</i>	-8.85	-6.95	-4.04	-2.68	-1.34	-0.64	-0.23
<i>D12S802</i>	-9.91	-1.98	-0.69	-0.23	0.09	0.14	0.10
<i>D12S799</i>	-16.09	-7.85	-6.07	-4.14	-2.09	-1.01	-0.36
<i>D12S297</i>	-0.08	-0.08	-0.06	-0.05	-0.03	-0.01	-0.00
<i>D12S303</i>	-15.30	-5.21	-2.81	-1.73	-0.73	-0.27	-0.06
<i>D12S296</i>	-6.12	-2.57	-1.31	-0.78	-0.32	-0.12	-0.03
<i>D12S300</i>	-7.60	-6.65	-5.78	-4.22	-2.31	-1.23	-0.51
<i>D12S807</i>	-8.99	-6.30	-3.70	-2.46	-1.30	-0.69	-0.30
<i>D12S834</i>	-17.97	-4.87	-2.48	-1.42	-0.49	-0.12	-0.01
13:							
<i>D13S250</i>	-6.53	-3.59	-1.97	-1.23	-0.54	-0.21	-0.05
<i>D13S252</i>	-9.35	-5.99	-3.73	-2.57	-1.38	-0.73	-0.30
<i>D13S305</i>	-5.55	-4.70	-2.99	-2.10	-1.17	-0.64	-0.28
<i>D13S242</i>	-15.33	-4.85	-2.35	-1.26	-0.35	-0.01	-0.36
<i>D13S258</i>	-5.30	-4.39	-2.27	-1.35	-0.55	-0.20	-0.04
<i>D13S628</i>	-3.18	-0.87	-0.26	-0.07	0.03	0.02	0.00
<i>D13S254</i>	0.22	0.21	0.19	0.15	0.09	0.04	0.01
<i>D13S248</i>	-6.84	-2.96	-1.45	-0.80	-0.24	-0.02	0.04
14:							
<i>D14S781</i>	-19.19	-8.22	-4.59	-3.00	-1.49	-0.71	-0.26
<i>D14S122</i>	-10.31	-1.58	0.24	0.79	0.96	0.74	0.36
<i>D14S121</i>	-10.50	-2.59	-1.15	-0.59	-0.15	0.01	0.05
<i>D14S562</i>	-12.38	-5.00	-2.25	-1.18	-0.36	-0.11	-0.06
<i>D14S119</i>	-7.11	-2.34	-1.03	-0.54	-0.16	-0.04	-0.01
<i>D14S140</i>	-15.56	-5.41	-3.01	-1.93	-0.93	-0.46	-0.19
<i>D14S553</i>	-3.55	0.46	0.94	0.96	0.70	0.37	0.12
<i>D14S118</i>	-11.44	-3.17	-1.54	-0.85	-0.27	-0.05	0.00
<i>D14S126</i>	0.20	0.19	0.14	0.09	0.03	0.01	0.01
<i>D14S131</i>	0.20	0.19	0.14	0.09	0.03	0.01	0.01
15:							
<i>D15S540</i>	-4.56	-1.01	-0.36	-0.12	0.04	0.08	0.06
<i>D15S537</i>	-10.62	-0.20	0.38	0.53	0.52	0.40	0.22
<i>D15S195</i>	-5.85	-4.90	-2.73	-1.75	-0.84	-0.39	-0.14
<i>D15S192</i>	-8.23	-5.90	-4.07	-2.79	-1.49	-0.77	-0.30
<i>D15S533</i>	-21.58	-7.39	-3.85	-2.35	-1.01	-0.39	-0.10
<i>D15S184</i>	-27.70	-5.42	-2.16	-0.96	-0.08	0.16	0.18
16:							
<i>D16S423</i>	-7.77	-1.39	-0.13	0.28	0.48	0.41	0.23
<i>D16S475</i>	-7.25	1.19	1.62	1.59	1.24	0.81	0.40

Table 4.1. Continued

Chromosome and Marker	LOD at $=\theta$						
	0.00	0.01	0.05	0.10	0.20	0.30	0.40
<i>D16S680</i>	-8.13	-2.19	-0.78	-0.26	0.07	0.13	0.09
<i>D16S683</i>	0.24	0.23	0.18	0.13	0.06	0.03	0.01
<i>D16S490</i>	-9.29	-2.02	-0.51	0.05	0.39	0.38	0.23
<i>D16S746</i>	-14.39	-3.91	-2.13	-1.26	-0.45	-0.09	0.03
<i>D16S487</i>	-19.07	-5.04	-2.23	-1.08	-0.15	0.16	0.18
<i>D16S671</i>	-3.95	-0.67	-0.02	0.20	0.33	0.31	0.19
<i>D16S676</i>	-15.29	-3.88	-1.34	-0.43	0.18	0.28	0.19
<i>D16S418</i>	-2.28	0.03	0.58	0.70	0.64	0.46	0.23
<i>D16S3024</i>	-14.67	-2.29	-0.42	0.21	0.54	0.49	0.29
<i>D16S291</i>	-8.42	-1.18	0.03	0.39	0.50	0.38	0.19
<i>D16S287</i>	-12.08	-3.13	-1.12	-0.36	0.17	0.28	0.21
17:							
<i>D17S695</i>	-11.97	-6.68	-3.70	-2.38	-1.13	-0.50	-0.16
<i>D17S919</i>	-4.85	-1.55	-0.82	-0.50	-0.21	-0.08	-0.02
<i>D17S900</i>	-15.94	-2.43	-0.97	-0.39	0.03	0.11	0.08
<i>D17S750</i>	-23.38	-4.43	-1.76	-0.74	0.02	0.22	0.19
<i>D17S515</i>	-16.07	-5.98	-3.08	-1.84	-0.72	-0.22	-0.01
<i>D17S722</i>	-9.99	-4.56	-2.45	-1.59	-0.86	-0.47	-0.20
<i>D17S914</i>	-10.53	-3.03	-1.36	-0.61	-0.01	0.14	0.10
18:							
<i>D18S818</i>	1.09	1.05	0.91	0.74	0.43	0.20	0.06
<i>D18S391</i>	-9.49	-4.01	-2.33	-1.48	-0.66	-0.27	-0.07
<i>D18S53</i>	-4.71	-0.67	-0.07	0.11	0.16	0.10	0.03
<i>D18S819</i>	-12.08	-6.23	-3.42	-2.22	-1.12	-0.56	-0.22
<i>D18S383</i>	-8.84	-2.44	-1.15	-0.66	-0.28	-0.12	-0.03
<i>D18S51</i>	-22.46	-6.36	-3.02	-1.72	-0.64	-0.22	-0.06
<i>D18S390</i>	-17.86	-4.77	-2.11	-1.09	-0.29	-0.01	0.04
<i>D18S380</i>	-11.53	-3.18	-1.34	-0.64	-0.11	0.08	0.10
<i>D18S64</i>	-24.62	-5.36	-2.58	-1.48	-0.60	-0.24	-0.08
19:							
<i>D19S549</i>	-5.52	-2.15	-1.28	-0.86	-0.45	-0.23	-0.09
<i>D19S395</i>	-27.00	-10.06	-5.72	-3.76	-1.89	-0.91	-0.33
<i>D19S403</i>	-4.81	-1.27	-0.65	-0.43	-0.24	-0.13	-0.06
<i>D19S400</i>	-5.79	-4.34	-2.19	-1.29	-0.53	-0.22	-0.09
<i>D19S393</i>	-2.57	-0.27	0.28	0.40	0.34	0.18	0.04
<i>D19S553</i>	-7.17	-1.68	-0.27	0.24	0.51	0.42	0.20
<i>D19S727</i>	-10.53	-7.24	-4.18	-2.69	-1.26	-0.55	-0.17
20:							
<i>D20S165</i>	-6.41	-3.01	-1.62	-0.96	-0.38	-0.14	-0.03
<i>D20S156</i>	-16.10	-6.37	-3.49	-2.27	-1.15	-0.57	-0.21
<i>D20S161</i>	-4.51	-1.22	-0.54	-0.27	-0.04	0.04	0.05

Table 4.1. Continued

Chromosome and Marker	LOD at $=\theta$						
	0.00	0.01	0.05	0.10	0.20	0.30	0.40
<i>D20S438</i>	-18.48	-4.85	-2.19	-1.17	-0.35	-0.07	0.00
<i>D20S423</i>	-19.72	-7.87	-4.30	-2.77	-1.36	-0.66	-0.24
<i>D20S428</i>	-10.24	-3.10	-1.72	-1.14	-0.59	-0.30	-0.11
<i>D20S149</i>	-6.98	-3.48	-1.94	-1.26	-0.61	-0.27	-0.08
<i>D20S94</i>	-18.96	-4.02	-2.00	-1.20	-0.50	-0.19	-0.04
<i>D20S164</i>	0.22	0.21	0.17	0.12	0.05	0.01	0.00
21:							
<i>D21S1414</i>	-5.14	-3.85	-2.30	-1.58	-0.86	-0.46	-0.19
<i>D21S1409</i>	-16.31	-8.05	-4.75	-3.11	-1.56	-0.77	-0.30
<i>D21S1245</i>	-5.06	-2.33	-1.30	-0.80	-0.33	-0.11	-0.02
<i>D21S1413</i>	-10.30	-4.63	-2.47	-1.57	-0.77	-0.38	-0.16
<i>D21S1246</i>	-5.43	-1.14	-0.50	-0.28	-0.10	-0.03	0.00
<i>D21S1411</i>	-14.02	-3.63	-1.93	-1.14	-0.59	-0.30	-0.11
22:							
<i>D22S533</i>	-5.92	-2.73	-1.74	-1.16	-0.53	-0.21	-0.05
<i>D22S528</i>	0.50	0.48	0.39	0.28	0.14	0.05	0.02
<i>D22S417</i>	-14.00	-7.52	-4.43	-2.99	-1.57	-0.80	-0.31
<i>D22S526</i>	-10.79	-4.84	-2.20	-1.19	-0.38	-0.07	0.02

NOTE.—Two-point linkage analyses were performed with the MLINK program of the FASTLINK\* package, under the assumptions of autosomal dominant inheritance and full penetrance. The disease-allele frequency was set at 0.0001.

\*Lathrop GM, Lalouel J-M, Julier C, Ott J (1984) Strategies for multilocus analysis in humans. PNAS 81:3443-3446.

Table 4.2. Results of the Multipoint Linkage Analysis

Position or Marker	Location Score
-49.9999	1.8770
-45.0000	2.0890
-40.0000	2.3220
-35.0000	2.5770
-30.0000	2.8550
-20.0000	3.4870
-15.0000	3.8420
-10.0000	4.2240
-5.0000	4.6330
-0.0001	5.0690
<b><i>D4S3038</i></b>	
0.0001	5.0690
0.1092	5.0710
0.2184	5.0740
0.3276	5.0760
0.4367	5.0790
0.5459	5.0820
0.6551	5.0840
0.7643	5.0870
0.8735	5.0890
0.9827	5.0920
1.0917	5.0940
<b><i>D4S114</i></b>	
1.0919	5.0940
1.1471	5.0950
1.2024	5.0960
1.2577	5.0960
1.3131	5.0970
1.3684	5.0980
1.4237	5.0990
1.4790	5.0990
1.5343	5.1000
1.5896	5.1010
1.6448	5.1010
<b><i>D4S43</i></b>	
1.6450	5.1010
1.7428	5.1010
1.8408	5.1010
1.9387	5.1010
2.0367	5.1010
2.1346	5.1010
2.2326	5.1010
2.3306	5.1010

Table 4.2. Continued

Position or Marker	Location Score
2.4285	5.1010
2.5265	5.1010
2.6243	5.1010
<b>D4S127</b>	
2.6245	5.1010
2.6909	5.1010
2.7573	5.1000
2.8237	5.1000
2.8902	5.1000
2.9566	5.0990
3.0231	5.0990
3.0895	5.0990
3.1559	5.0980
3.2224	5.0980
3.2887	5.0980
<b>D4S412</b>	
3.2889	5.0980
8.2888	4.6600
13.2888	4.2500
18.2888	3.8670
23.2888	3.5100
28.2888	3.1800
33.2888	2.8760
38.2888	2.5960
43.2888	2.3400
48.2888	2.1050
53.2887	1.8920

NOTE.—Multipoint linkage analysis was performed using SimWalk\*, with markers on the short arm of chromosome 4, under the assumptions of dominant inheritance and a disease allele frequency of 0.001.

\*Sobel E and Lange K (1996) Descent graphs in pedigree analysis: applications to haplotyping, location scores, and marker sharing statistics. *Am J Hum Genet* 58:1323-1337.

## APPENDIX A

### DISTAL ARTHROGRYPOSIS TYPE 5 IS

### CAUSED BY DEFECTS OF MYOSIN

The following abstract, coauthored by myself, Lynn B. Jorde, and Michael J. Bamshad, was presented at the 2006 annual meeting of the American Society of Human Genetics held in New Orleans and published in the *American Journal of Human Genetics* in 2006 (volume 76, Supplement, page 74).

## Distal arthrogryposis type 5 is caused by defects of myosin

Toydemir R<sup>1</sup>, Jorde LB<sup>1</sup>, Bamshad M<sup>2,3</sup>

<sup>1</sup>Department of Human Genetics, University of Utah, Salt Lake City, UT

<sup>2</sup>Departments of Pediatrics and Genome Science, University of Washington, Seattle,

WA <sup>3</sup>Children's Hospital and Regional Medical Center, Seattle, WA

The distal arthrogryposes (DA) are a group of syndromes characterized by congenital contractures of the hands and feet, limited proximal joint involvement, autosomal dominant inheritance, reduced penetrance, and variable expressivity. To date, 10 different DA syndromes have been characterized. Among the DAs, DA5 is unique since in addition to contractures of the skeletal muscles, affected individuals have ocular abnormalities such as ptosis, ophthalmoplegia, and strabismus. Based on our previous findings, which showed DAs are caused by mutations that encode proteins of contractile apparatus of myofibers, we hypothesized that DA5 might be caused by contractile proteins that are expressed in both skeletal and extraocular muscles. Two such proteins are myosin heavy chain IIa and myosin heavy chain 13 that are encoded by *MYH2* and *MYH13*, respectively. We screened the entire coding region of these genes in 8 independent cases of DA5. In two cases, we found missense mutations in *MYH2* that caused substitutions of highly conserved amino acid residues. Neither of these mutations was found in more than 200 chromosomes from controls matched for geographic ancestry. Additionally, one of the two DA5 cases with a *MYH2* mutation also had a mutation in *MYH13*. This mutation also alters a highly conserved amino acid

residue and it is not found in the healthy population. Our results suggest that DA5 is genetically heterogeneous, and mutations in *MYH2* cause a subset of DA5 cases. In addition, mutations in other contractile proteins might modify the phenotype associated with *MYH2* mutations or, alternatively, *MYH2* might in some cases modify a phenotype caused by mutations in genes that encode other contractile proteins.



## APPENDIX B

### A NEW AUTOSOMAL DOMINANT DISTAL ARTHROGRYPOSIS SYNDROME CHARACTERIZED BY PLANTAR TENDON CONTRACTURES IN A LARGE UTAH KINDRED MAPS TO 2q

The following abstract, coauthored by myself, David A. Stevenson, Kathryn Swoboda, Hilary Coon, and Michael J. Bamshad, was presented at the 2006 annual meeting of the American Society of Human Genetics held in New Orleans and published in the *American Journal of Human Genetics* in 2006 (volume 76, Supplement, page 282).

A new autosomal dominant distal arthrogryposis syndrome characterized by plantar tendon contractures in a large Utah kindred maps to 2q

Stevenson DA<sup>1</sup>, Toydemir R<sup>2</sup>, Swoboda K<sup>1,3</sup>, Coon H<sup>4</sup>, Bamshad M<sup>5</sup>

Departments of <sup>1</sup>Pediatrics, <sup>2</sup>Human Genetics, <sup>3</sup>Neurology, and <sup>4</sup>Psychiatry (Neurodevelopmental Genetics Program), University of Utah, Salt Lake City, UT

<sup>5</sup>Department of Pediatrics, University of Washington, Seattle, WA

The distal arthrogryposis (DA) syndromes are a distinct group of disorders characterized by contractures of two or more different body areas. More than a decade ago, we revised the classification of DAs and distinguished several new syndromes. This classification facilitated the identification of nearly half a dozen genes (i.e., *TNNI2*, *TNNT3*, *MYH3*, *MYH8*, and *TPM2*) that encode components of the contractile apparatus of fast-twitch myofibers and when defective cause DA. We now report the characterization of a novel DA disorder in a large five-generation Utah family in which plantar tendon shortening was transmitted among 14 affected individuals in an autosomal dominant pattern. Contractures of hips, elbows, wrists, and fingers varied in severity among affected individuals. All affected individuals had normal neurological examinations; electromyography and creatinine kinase levels on selected individuals were normal. We have tentatively labeled this condition distal arthrogryposis type 10 (DA10). A genome-wide linkage scan showed a maximum LOD score of 3.96 at marker D2S364 on chromosome 2q near a region containing several genes that encode contractile proteins.